*Current Research (2014) Newfoundland and Labrador Department of Natural Resources Geological Survey, Report 14-1, pages 99-128*

# LATE NEOPROTEROZOIC EPITHERMAL ALTERATION AND MINERALIZATION IN THE WESTERN AVALON ZONE: A SUMMARY OF MINERALOGICAL INVESTIGATIONS AND NEW U/Pb GEOCHRONOLOGICAL RESULTS

G.W. Sparkes and G.R. Dunning[1]
Mineral Deposits Section
[1]Department of Earth Sciences, Memorial University, St. John's, NL, A1B 3X5

**ABSTRACT**

*Investigations into the distribution and mineralogy of late Neoproterozoic epithermal alteration systems of the western Avalon Zone, using visible/infrared spectroscopy (VIRS), provide new information that allows for better definition of spatial zonation patterns at select occurrences. The alteration zones contain alunite, pyrophyllite, dickite, kaolinite and diaspore, and the distribution of these minerals, coupled with compositional variations in alunite and the crystallinity of white micas, locally suggests variations in fluid temperatures. However, systematic spatial zonation cannot be defined in all examples.*

*The U/Pb geochronological investigations reveal an age of 635 ± 2 Ma for a granitic intrusion on the southern Burin Peninsula, representing a previously unrecognized magmatic episode in the western Avalon Zone. A sample from a unit previously mapped as part of the* ca. *550 Ma Cross Hills Intrusive Suite instead gave an age of 581 ± 1.5 Ma, indicating the presence of older plutonic rocks that are not fully defined by existing mapping. At the Stewart prospect, quartz diorite affected by advanced argillic alteration and related mineralization gave an age of 577 ± 1.4 Ma, and a nearby granodiorite (part of a unit referred to as the Burin Knee granite) gave an age of 575.5 ± 1 Ma; both of these ages are close (within error range) to the 577 ± 3 Ma age previously reported for the Swift Current Granite. Felsic volcanic rocks of the Marystown Group were dated at 576.8 ± 2.6 Ma on the southern Burin Peninsula, and at 576.2 ± 2.8 Ma in the vicinity of Tower prospect at the northern end of the Burin Peninsula. New analyses of the archived zircon, derived from a sample of felsic ash-flow tuff from the Marystown Group that had previously given an age of* ca. *608 Ma, suggest that the older result reflects inheritance, and the revised crystallization age is 574.4 ± 2.5 Ma. Collectively, these new geochronological data emphasize the importance of the period from* ca. *580 to 570 Ma for volcanic and plutonic activity throughout this region; further, it suggests that epithermal-style alteration and mineralization were broadly synchronous with this activity.*

## INTRODUCTION

The Avalon Zone of Newfoundland hosts well-preserved examples of high- and low-sulphidation epithermal systems that are amongst some of the oldest known in the world. These Neoproterozoic epithermal systems occur throughout the Avalon Zone and related terrains, from the Carolina Slate Belt in the south to the Avalon Peninsula of Newfoundland in the north, where the Avalon Zone forms the northeastern terminus of the eastern margin of the Appalachian orogen (Williams, 1979; O'Brien *et al*., 1996, 1998). Several past-producing epithermal gold deposits, and their surrounding areas, are currently being reevaluated through exploration (*e.g.*, Hope Brook in Newfoundland and Haile in the Carolina Slate Belt). The most extensive and numerous examples of epithermal alteration systems in Newfoundland are located within the western Avalon Zone, namely the Burin Peninsula region, and the exploration potential of many of these examples remains largely untested in the subsurface.

The western Avalon Zone of Newfoundland has long been known to host examples of high-sulphidation-style epithermal alteration and related mineralization, which locally contain significant gold mineralization variably associated with silver, copper, arsenic, antimony and zinc (*e.g.,* Dubé *et al*., 1998; O'Brien *et al*., 1998, 1999). Individual belts of advanced argillic alteration related to the formation of these high-sulphidation systems can be traced intermittently along strike for up to 16 km on the Burin Peninsula. These alteration zones contain variably developed assemblages including pyrophyllite, alunite, mus-

covite, illite and locally topaz, diaspore and lazulite. The spatial distribution of the various alteration minerals remains poorly understood, and such information is valuable to establish the depth of erosion within these epithermal systems.

More recently, low-sulphidation-style chalcedonic silica veins and related breccias have been recognized within the western Avalon Zone. Several of these zones are auriferous (Seymour, 2006; Evans and Vatcher, 2010; Sparkes, 2012 and references therein). In the northern portion of the western Avalon Zone, exploration in the vicinity of the Big Easy prospect has identified low-sulphidation gold mineralization hosted within sedimentary rocks of the Musgravetown Group, potentially representing some of the youngest mineralization in the region. The preservation of surface and near-surface features, such as the deposition of silica gels within a lacustrine environment (Silver Spruce website, 2013), illustrate the exceptional preservation of these Neoproterozoic epithermal systems.

This report highlights two aspects of epithermal mineralization in the region. The first focuses on the mineralogy and distribution of the hydrothermal alteration assemblages at several prospects, and is the first investigation of these systems by the Geological Survey of Newfoundland and Labrador using a portable visible infra-red reflectance spectrometer (VIRS; TerraSpec® Pro). This instrument has the capability to identify the cryptic alteration minerals associated with various styles of epithermal systems and allows them to be mapped in detail. The interpretation of the spectra collected from field samples is provided by TSG™ Pro software, which identifies the two most dominant minerals, based on distinct spectral characteristics. Results from automated software are confirmed and augmented through manual interpretation of the data using reference spectra for known minerals. For a more detailed discussion of the methods and description of the portable reflectance spectrometer, *see* Kerr *et al*. (2011).

Geochronological sampling carried out as part of this study has produced several U/Pb zircon ages that provide constraints on the development of these epithermal systems, and are also relevant to the regional geology. The second part of this report summarizes these results and their interpretation.

## REGIONAL GEOLOGY OF THE WESTERN AVALON ZONE

The Avalon Zone is characterized by widespread magmatic activity ranging in age from *ca.* 760–550 Ma (O'Brien *et al*., 1996) that occurred within arc, or arc-adjacent and continental extensional settings (O'Brien *et al*., 1999). Within the volcanic sequences, high-level intrusions generated regional-scale magmatic–hydrothermal systems that were locally accompanied by precious-metal deposition (O'Brien *et al*., 1999). Most of the epithermal alteration and related mineralization currently identified in the Avalon Zone is hosted by subaerial felsic volcanic rocks ranging in age from 590–550 Ma. These volcanic rocks are intercalated with, and overlain by, sequences of marine, deltaic and fluviatile siliciclastic sedimentary rocks. The deposition of these sedimentary sequences can locally be demonstrated to have played a vital role in the preservation of the underlying epithermal systems through rapid burial (*e.g.,* Sparkes *et al*., 2005).

Late Neoproterozoic rocks are, in turn, overlain by a Cambrian platformal sedimentary cover sequence that postdates the waning of volcanic activity and related epithermal systems (O'Brien *et al*., 1996 and references therein). The Neoproterozoic rocks, and Cambrian cover sequences, are unconformably overlain by isolated outliers of Late Silurian to Early Devonian terrestrial volcanic and sedimentary rocks (O'Brien *et al*., 1995). The intensity of Paleozoic deformation broadly increases from east to west toward the Dover and Hermitage Bay faults, which mark the western extent of Avalonian rocks and defines their tectonic contact with the adjacent Gander Zone (Blackwood and Kennedy, 1975; Kennedy *et al*., 1982). Thus, epithermal systems in the western Avalon Zone are generally more strongly deformed than those farther to the east. Most of the deformation is attributed to the Devonian Acadian orogeny (Dallmeyer *et al*., 1983; Dunning *et al*., 1990; O'Brien *et al*., 1991, 1999; van Staal, 2007); however, evidence for an older, Precambrian deformational event, is also locally preserved (*e.g.,* Anderson *et al.*, 1975; O'Brien, 1993, 2002; O'Brien *et al*., 1996).

Epithermal-style alteration and mineralization is most abundant in volcanic rocks of the 590–570 Ma Marystown Group (Strong *et al*., 1978a, b; O'Brien *et al*., 1999). This sequence comprises greenschist-facies subaerial flows, and related pyroclastic and volcaniclastic rocks. The volcanic rocks range in composition from basalt, through andesite and rhyodacite, to rhyolite and are of both calc-alkaline and tholeiitic affinity (Hussey, 1979; O'Brien *et al*., 1990, 1996, 1999). The Marystown Group occupies the core of the Burin Peninsula, forming a broad-scale anticlinorium, which is flanked to the east by a shoaling-upward sequence of marine to terrestrial sedimentary rocks of the Neoproterozoic Musgravetown Group (O'Brien, *et al*., 1999; Figure 1); volcanic rocks at the base of the Musgravetown Group (Bull Arm Formation) are dated at 570 +5/-3 Ma (O'Brien *et al*., 1989).

To the west and north, the Marystown Group is overlain by the *ca.* 570 to 550 Ma Long Harbour Group. The Long

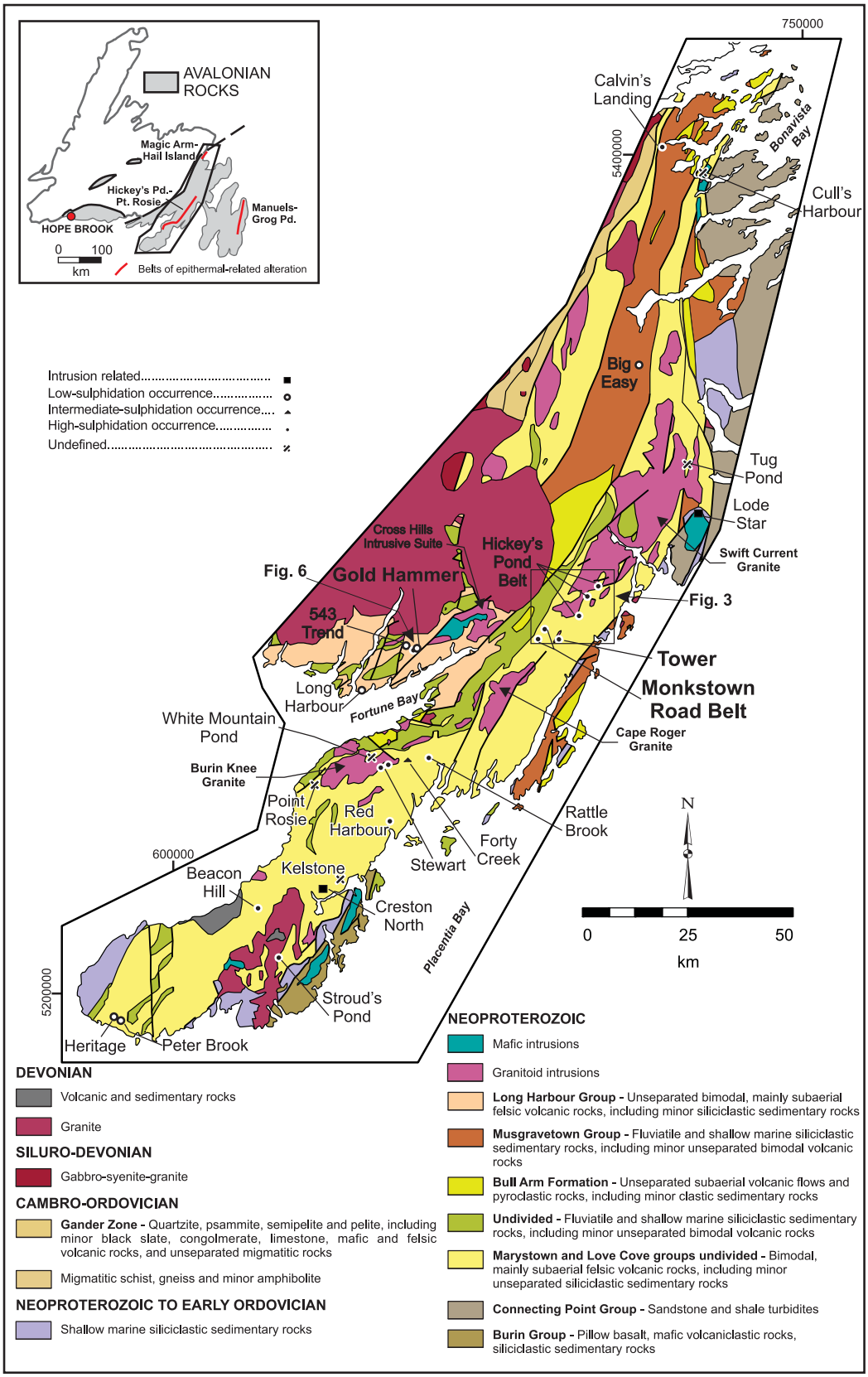


**Figure 1.** *Regional geology map of the western Avalon Zone outlining the distribution of known epithermal prospects (modified from O'Brien* et al.*, 1998; coordinates are listed in NAD 27, Zone 21).*

Harbour Group is dominated by subaerial felsic volcanic rocks of alkaline to peralkaline affinity along with lesser mafic volcanic rocks and siliciclastic sedimentary rocks, which pass conformably upward into fossiliferous Cambrian sedimentary rocks related to the development of a platformal cover sequence (Williams, 1971; O'Brien, *et al*., 1984; 1995). The Long Harbour Group is divisible into a lower volcanic sequence (Belle Bay Formation) and an upper volcanic sequence (Mooring Cove Formation), which are separated by a clastic sedimentary unit known as the Anderson's Cove Formation (O'Brien *et al*., 1984). Rhyolites from both the Belle Bay and Mooring Cove formations have been dated at 568 ± 5 and 552 ± 3, respectively (O'Brien *et al*., 1994).

Several high-level granitoid plutons intrude along the western margin of the Avalon Zone in Newfoundland. On the Burin Peninsula these form a broad, semi-continuous, north-northeast-trending belt consisting of hornblende–biotite granite, diorite and gabbro (Figure 1). The largest of these bodies, the Swift Current Granite (Figure 1) is locally dated at 577 ± 3 Ma (O'Brien *et al.*, 1998), and others, including the Cape Roger granite and the 'Burin Knee granite', are inferred to be coeval Precambrian intrusions (O'Brien and Taylor, 1983; O'Brien *et al*., 1984). North of Fortune Bay, the Long Harbour Group is intruded by the Cross Hills Intrusive Suite, which has a preliminary age of 547 +3/-6 Ma and hosts Zr–Nb–REE mineralization (Tuach, 1991). This intrusion represents one of the youngest magmatic events prior to the cessation of hydrothermal activity within the region. The youngest plutonic rocks in the area are Devonian (Ackley and St. Lawrence granites), and other small plutonic units of undeformed character are inferred to be of this age.

## MAPPING OF SELECTED ALTERATION ZONES

The spectral features of individual minerals can be used as potential vectors within zones of epithermal alteration. For instance, VIRS can be used to distinguish between potassic- and sodic-dominated alunite (Thompson *et al.*, 1999). The latter is typically associated with higher temperatures of the hydrothermal system that potentially host ore-grade mineralization (*e.g.,* Chang *et al*., 2011; Stoffregen and Cygan, 1990).

Spectral variations within white micas can also be used in a similar fashion to identify areas of higher temperatures within the hydrothermal system. The parameter of interest is termed white-mica crystallinity (WMC). The classification of the white mica composition is largely based on the position of the AlOH absorption feature at ~2200 nm; paragonite generally displays values around 2184 nm, whereas muscovite has values around 2190 nm and phengite has values around 2225 nm (AusSpec, 2008a; Figure 2). The WMC for a particular white mica phase is defined as the depth of the AlOH feature at ~2200 nm divided by the depth of the water feature at 1900 nm on a hull quotient spectrum (AusSpec, 2008b; Figure 2); however, some caution must be used in applying this technique, because if the sample being analyzed contains a large amount of chalcedonic quartz, which contains a water feature within its spectra, in addition to white mica, this will result in a larger $H_2O$ feature in the spectra, which will, in turn, result in a lower calculated WMC value for the sample. Generally, a WMC value of <1 implies a low crystallinity and a value >1 records a higher crystallinity (AusSpec, 2008b), which implies a higher temperature of formation; however, such values need to be checked against individual datasets. Observations from areas investigated during this study indicate that white mica alteration associated with high-temperature hydrothermal alteration produce WMC values ranging from >2 (*e.g.,* Monkstown Road Belt and Tower prospect) to >3 (*e.g.,* Gold Hammer prospect), and values below this are inferred

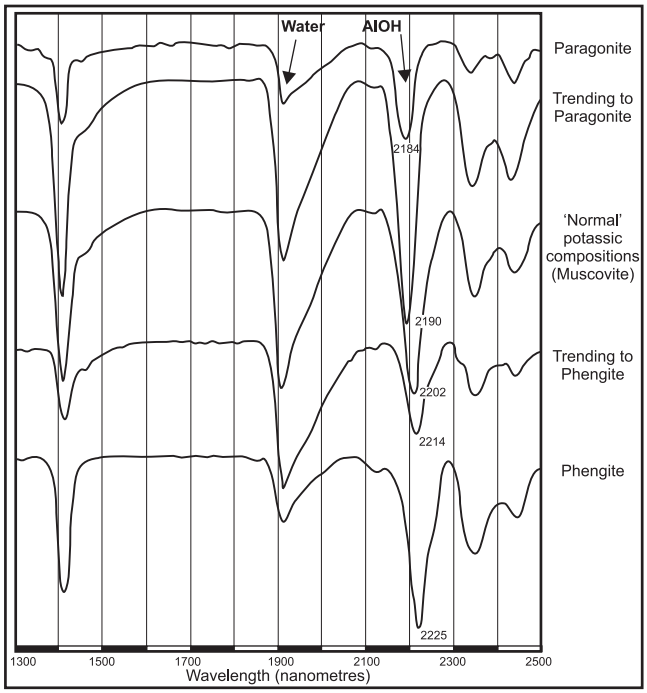


**Figure 2.** *Spectra for select white mica phases showing the characteristic shift in the AlOH feature, located at ~2200 nm (modified from AusSpec, 2008a). Also shown is the location of the water feature used in the calculation of the white mica crystallinity. Note highly crystalline white micas (*i.e.*, 2M white micas) can be referred to by their mineral names muscovite, phengite or paragonite. The illitic white micas also display compositional substitution and can be referred to as illite, phengitic illite or paragonitic illite (AusSpec, 2008a).*

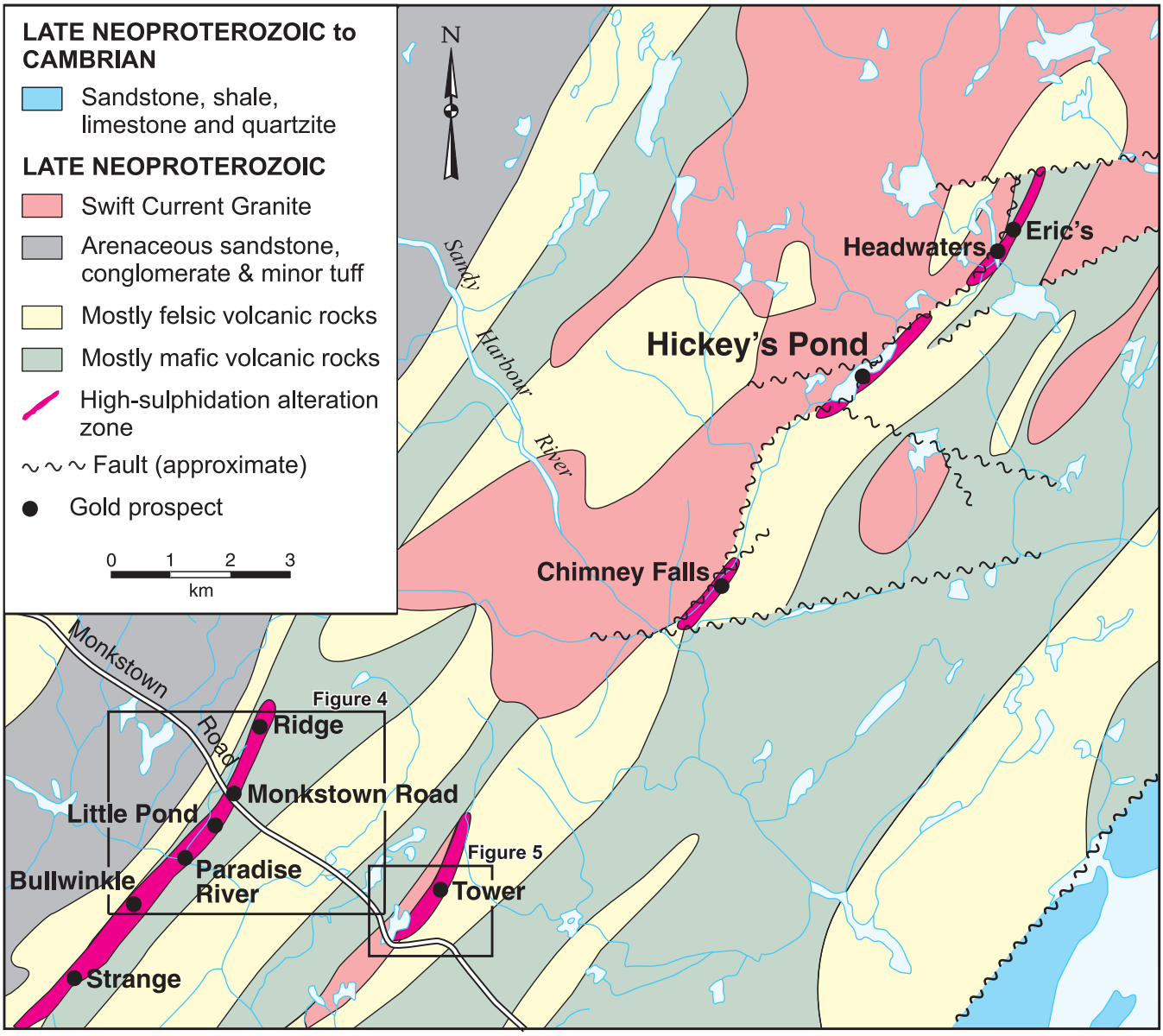


**Figure 3.** *Regional geology map of the high-sulphidation related alteration in the vicinity of Monkstown Road and Hickey's Pond prospects (*from *Huard and O'Driscoll, 1986; modified from O'Brien* et al.*, 1999).*

to represent background regional alteration. These, and other mineralogical parameters, are applied below to test whether or not any zonation can be identified within the hydrothermal alteration in the study area. These zones lack diamond drilling and the study is limited to surface sampling; however, sufficient local topography provides some insight into the vertical distribution of the alteration.

## MONKSTOWN ROAD BELT

The Monkstown Road prospect (Huard and O'Driscoll, 1985, 1986; Huard, 1990) is the main prospect within the Monkstown Road alteration belt (Figure 3), which was first noted by Tuach (1984). The Monkstown Road prospect is well-known for the presence of the bright blue phosphate mineral lazulite ($MgAl_2(PO_4)_2(OH)_2$; Plate 1). Lazulite occurs within quartz–specularite veins that are developed within an extensive northeast–southwest-trending zone of advanced argillic alteration containing alunite, pyrophyllite, specularite and lesser dickite. The host rocks to the alteration belong to the Marystown Group, and are locally strongly foliated. Similarly, the zones of advanced argillic alteration display an intense penetrative fabric outside of areas that have been strongly silicified.

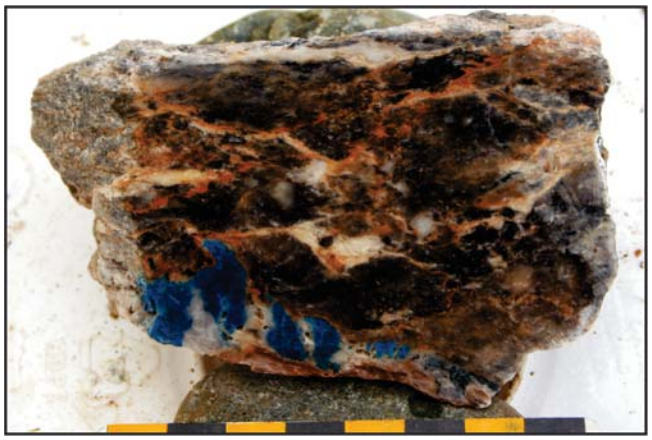

**Plate 1.** *Blue lazulite occurring within quartz–specularite–pyrophyllite–alunite–dickite alteration; Monkstown Road prospect.*

The Monkstown Road area has been the focus of intermittent mineral exploration and scientific studies (*e.g.,* Saunders and Reusch, 1984; Degagne and Robertson, 1985; Huard and O'Driscoll, 1985, 1986; Dimmell and MacGillivray, 1989; Huard, 1990; Sexton *et al*., 2003; Dyke, 2007, 2009; Dyke and Pratt, 2008; Labonte, 2010), partly due to the fact that the alteration zone resembles the auriferous advanced argillic alteration at the Hickey's Pond prospect to the northeast (Saunders and Reusch, 1984; Huard and O'Driscoll, 1985; O'Brien *et al.,* 1999*;* Figure 3). The Hickey's Pond prospect is locally host to grab samples assaying up to 31 g/t Au, 110 g/t Ag along with anomalous As, Bi, Cu, Sb, Se, Te, and Hg (Table 1) in association with vuggy silica zones within more extensive sodic-alunite alteration (O'Brien *et al.,* 1999; *this study*). Advanced argillic alteration at Monkstown Road is largely barren, with only localized anomalous gold values of up to 1.18 g/t (Saunders and Reusch, 1984). Higher grade mineralization assaying up to 8.16 g/t Au (Degagne and Robertson, 1985) has been reported for the muscovite–pyrite alteration developed adjacent to the alunite–pyrophyllite–specularite alteration at the Monkstown Road prospect; however subsequent attempts to duplicate this result have failed to produce similar values.

Spectrometer studies of the alteration throughout the Monkstown Road Belt show the dominance of alunite alteration and lesser zones of pyrophyllite at the Monkstown Road, Monkstown Road South and Ridge prospects (Figure 4). Spectral data collected from the main Monkstown Road prospect show the alteration is dominated by pyrophyllite and lesser alunite and dickite, despite the abundance of a pinkish alteration mineral throughout the outcrop, which elsewhere in the region has previously been used as an indication of alunite. From the limited data, it appears that areas of lower elevation (*e.g.,* Little Pond and Paradise River prospects; <87 m elevation) are dominated by potassic alunite, whereas the remainder of the alteration zone exposed at higher elevations (>125 m) is dominated by sodic alunite. Earlier work using a different type of spectrometer identified topaz, indicating high temperatures of formation (>260° C, Reyes, 1990) at the Little Pond prospect (Figure 4); however, in contrast to the sampling carried out the exploration data classify the alunite at that location as natroalunite (sodic alunite; Sexton *et al*., 2003) as opposed to potassic alunite.

The alteration zone was mapped as far north as the Ridge prospect, where a prominent north–south-trending linear suggests that it may be truncated. The alteration zone is inferred to extend to the southwest beyond the current limit of mapping toward the area of the Strange prospect (Figure 3). These occurrences combine to give an overall strike length of up to 5 km, along which anomalous gold mineralization is locally identified (Huard and O'Driscoll, 1986; Huard, 1990; Sexton *et al.*, 2003). However, sampling of the Monkstown Road Belt failed to identify any significant enrichment of gold or silver (Table 1).

Outside of the main advanced argillic alteration zone, the host rocks primarily consist of mafic to intermediate and felsic crystal tuffs. Figure 4 displays the regional geology of the area as portrayed by Huard and O'Driscoll (1986). It should be noted however that more detailed property-scale mapping, such as that conducted by Hayes (2000), demonstrates an increased abundance of felsic volcanic rocks in the area compared to what is shown on regional scale maps. Spectral results from the surrounding country rock suggest iron–magnesium chlorite in the mafic units, and phengite in felsic units (Figure 4); these minerals are inferred to be part of the regional metamorphic assemblage, as similar results were obtained elsewhere in the Burin Peninsula region. The zone of advanced argillic alteration, which can locally be inferred to be up to 200 m wide, occurs within a moderate magnetic low flanked to the east and west by magnetic highs (Hayes, 2000). It is bounded to the east and west by muscovite–pyrite-bearing shear zones displaying local evidence for a reverse sense of motion, with thrusting toward the east (O'Brien *et al*., 1999). These shear zones have a WMC of >2, indicating high temperatures of formation, and are commonly strongly foliated and highly friable (Plate 2). Similar values are obtained for analogous alteration along strike to the northwest in the vicinity of the Ridge prospect, which may represent the strike extension of this structure.

## TOWER PROSPECT

Approximately 4 km to the east-southeast of the Monkstown Road Belt is a second subparallel belt of advanced argillic alteration, referred to as the Tower

**Table 1.** Geochemical samples collected in relation to mapping of select zones of advanced argillic alteration; also included are representative samples from the Hickey's Pond prospect for comparison. Note: N/A = not analyzed; - = below detection limit; coordinates are listed in NAD27, Zone 21

| Sample | UTM E | UTM N | Prospect | Description | Alteration Mineralog y | SiO2 | Al2O3 | Fe2O3 | Fe2O3 | FeO | MnO | MgO | CaO | Na2O | K2O | TiO2 |
|---|---|---|---|---|---|---|---|---|---|---|---|---|---|---|---|---|
| | | | | | | % | % | Total % | % | % | % | % | % | % | % | % |
| | | | | | Detection limit | 0.01 | 0.01 | 0.01 | 0.01 | 0.01 | 0.01 | 0.01 | 0.01 | 0.01 | 0.01 | 0.001 |
| GS-11-02 | 688612 | 5287616 | Monkstown Road | strongly foliated quartz-white mica schist | Muscovite | 78.82 | 10.98 | 1.75 | - | - | 0.009 | 0.45 | 0.01 | 0.10 | 3.52 | 0.357 |
| GS-11-03 | 688869 | 5287480 | Monkstown Road | chlorite schist | FeMgChlorite,Epidote | 52.75 | 16.68 | 9.63 | 6.70 | 2.64 | 0.215 | 2.58 | 6.80 | 2.53 | 1.20 | 1.186 |
| GS-11-04 | 688801 | 5287550 | Monkstown Road | silicification with minor hydrothermal brecciatior | Pyrophyllite | 95.40 | 1.01 | 2.01 | 1.88 | 0.12 | - | - | 0.02 | - | - | 0.693 |
| GS-11-05 | 688787 | 5287534 | Monkstown Road | massive pinkish silica-specularite alteration | | 94.58 | 1.07 | 1.07 | 0.35 | 0.64 | 0.005 | 0.07 | 0.08 | - | 0.08 | 0.708 |
| GS-11-10 | 688906 | 5287746 | Monkstown Road | quartz-pyrite alteration | Na Alunite | 71.31 | 11.63 | 1.91 | 0.23 | 1.51 | - | - | 0.08 | 1.22 | 1.46 | 0.466 |
| GS-11-11 | 688901 | 5287762 | Monkstown Road | alunite-specularite alteration | Na Alunite | 78.74 | 8.57 | 2.31 | - | - | - | - | 0.08 | 0.96 | 0.86 | 0.425 |
| GS-11-13 | 689045 | 5287704 | Monkstown Road | intense pyrite-chlorite alteration | FeMgChlorite,Epidote | 56.92 | 17.46 | 7.67 | 2.66 | 4.50 | 0.183 | 1.53 | 5.53 | 5.61 | 0.23 | 1.134 |
| GS-11-84 | 689563 | 5288348 | Ridge | white mica-pyrite alteration | Muscovite | 66.74 | 15.70 | 3.85 | 3.24 | 0.55 | 0.086 | 2.09 | 0.24 | 0.29 | 4.08 | 0.581 |
| GS-11-86 | 689577 | 5288500 | Ridge | quartz-alunite alteration | Na Alunite | 58.81 | 16.92 | 0.22 | 0.05 | 0.15 | - | - | 0.04 | 2.13 | 1.25 | 0.473 |
| GS-11-87 | 689564 | 5288520 | Ridge | sheared white mica- pyrite alteration | Muscovite | 61.26 | 17.68 | 6.28 | 1.37 | 4.42 | 0.060 | 1.77 | 0.19 | 0.67 | 3.80 | 1.203 |
| GS-11-112 | 689135 | 5288184 | Ridge | white mica-pyrite alteration | Paragonitic Illite,Montmorillonite | 66.95 | 15.42 | 6.30 | 6.13 | 0.15 | 0.041 | 1.79 | - | 0.80 | 2.94 | 1.483 |
| GS-11-114 | 689203 | 5288327 | Ridge | fine-grained, grey-green siliceous mafic volcanic | Epidote,FeMgChlorite | 66.32 | 12.71 | 5.59 | 3.49 | 1.89 | 0.143 | 2.13 | 5.98 | 2.88 | - | 0.747 |
| GS-11-115 | 689203 | 5288327 | Ridge | silica-pyrite alteration | Phengite,Epidote | 66.01 | 18.04 | 2.50 | 2.29 | 0.18 | 0.025 | 0.31 | 1.28 | 7.45 | 1.44 | 0.223 |
| GS-11-125 | 688309 | 5286941 | Little Pond | chlorite-pyrite alteration | FeMgChlorite,Muscovite | 56.87 | 15.26 | 7.72 | 2.29 | 4.89 | 0.096 | 4.36 | 1.45 | 4.17 | 1.20 | 0.945 |
| GS-11-126 | 688283 | 5286937 | Little Pond | silica-hematite alteration | K Alunite | 51.92 | 19.20 | 0.26 | - | - | - | - | 0.02 | 1.18 | 3.25 | 0.158 |
| GS-11-127 | 688134 | 5286601 | Paradise River | alunite-specularite alteration | K Alunite | 66.64 | 13.71 | 1.14 | 1.09 | 0.05 | - | - | 0.06 | 0.63 | 2.19 | 0.503 |
| GS-11-466 | 687453 | 5285768 | Bullwinkle | brecciated alunite alteration with hematite-rich matrix | Na Alunite,Phengite | 89.03 | 2.90 | 2.17 | 1.82 | 0.32 | 0.002 | - | 0.02 | 0.05 | 0.21 | 0.489 |
| GS-11-470 | 687749 | 5285874 | Bullwinkle | grey silica alteration with fine-grained disseminated pyrite | FeMgChlorite | 77.72 | 9.54 | 2.85 | - | - | 0.025 | - | 1.05 | 3.12 | 2.55 | 0.196 |
| GS-11-134 | 692357 | 5286163 | Tower | 2.5 m chip sample across alunite-specularite alteration | Na Alunite | 67.59 | 16.28 | 5.45 | 3.27 | 1.96 | 0.002 | 0.03 | 0.12 | 0.53 | 1.42 | 0.952 |
| GS-11-136 | 692347 | 5286177 | Tower | silica alteration | Na Alunite | 59.14 | 15.70 | 0.21 | 0.10 | 0.10 | - | - | 0.05 | 2.02 | 1.52 | 0.518 |
| GS-11-138A | 692347 | 5286177 | Tower | alunite-pyrite alteration | Na Alunite | 66.58 | 10.70 | 3.24 | - | - | 0.002 | 0.01 | 0.08 | 1.48 | 0.87 | 0.386 |
| GS-11-138B | 692347 | 5286177 | Tower | alunite-specularite alteration | Na Alunite,Pyrophyllite | 67.10 | 10.82 | 3.84 | 3.79 | 0.05 | 0.003 | 0.02 | 0.09 | 1.55 | 0.85 | 0.401 |
| GS-11-139 | 692365 | 5286192 | Tower | alunite-specularite alteration | Na Alunite,Muscovite | 66.73 | 13.80 | 3.12 | 3.04 | 0.07 | 0.002 | - | 0.06 | 0.97 | 0.81 | 0.493 |
| GS-11-140 | 692365 | 5286192 | Tower | alunite-specularite alteration | Na Alunite | 44.08 | 24.73 | 2.04 | - | - | 0.001 | - | 0.11 | 2.34 | 1.40 | 0.459 |
| GS-11-144 | 692423 | 5286147 | Tower | white mica-pyrite alteration | Na Alunite,Dickite | 65.91 | 13.89 | 3.13 | 0.83 | 2.08 | - | - | 0.05 | 1.14 | 0.81 | 0.480 |
| GS-11-145 | 692429 | 5286163 | Tower | beige silica-pyrite alteration | | 60.51 | 15.00 | 2.36 | 0.58 | 1.60 | - | - | 0.03 | 1.11 | 1.69 | 0.574 |
| GS-11-147 | 692411 | 5286162 | Tower | quartz-white mica-specularite alteration | Muscovite | 64.73 | 16.16 | 8.66 | 8.53 | 0.12 | 0.005 | 0.10 | 0.29 | 0.11 | 4.35 | 1.186 |
| GS-11-154 | 692433 | 5286427 | Tower | medium-grained, epidote altered granodiorite | Epidote,Phengite | 62.75 | 15.78 | 4.73 | 2.93 | 1.62 | 0.152 | 1.50 | 4.84 | 4.04 | 1.79 | 0.675 |
| GS-12-29 | 692664 | 5286246 | Tower | white mica alteration | Phengite | N/A | N/A | N/A | N/A | N/A | N/A | N/A | N/A | N/A | N/A | N/A |
| GS-12-88 | 691772 | 5285374 | Tower | white mica-pyritic alteration | Phengite | 71.13 | 15.69 | 3.57 | 1.98 | 1.43 | 0.071 | 0.86 | 0.10 | 3.01 | 2.81 | 0.472 |
| GS-12-89 | 692000 | 5285778 | Tower | alunite-pyrite alteration | Na Alunite | N/A | N/A | N/A | N/A | N/A | N/A | N/A | N/A | N/A | N/A | N/A |
| GS-12-221 | 692510 | 5286126 | Tower | white mica-pyrite alteration | Phengite | N/A | N/A | N/A | N/A | N/A | N/A | N/A | N/A | N/A | N/A | N/A |
| GS-11-359 | 658959 | 5282651 | Gold Hammer | beige silica alteration | Paragonite | 82.46 | 10.73 | 0.26 | 0.11 | 0.14 | - | - | - | 0.08 | 2.88 | 0.197 |
| GS-11-362 | 658986 | 5282489 | Gold Hammer | purple, flow-banded rhyolite | Phengite | 75.96 | 11.41 | 2.65 | 2.42 | 0.21 | 0.006 | 0.03 | 0.03 | 4.36 | 2.97 | 0.193 |
| GS-11-364 | 658870 | 5282568 | Gold Hammer | silica alteration | Paragonite | 96.59 | 1.97 | 0.76 | - | - | - | - | - | - | 0.49 | 0.204 |
| GS-11-365 | 658829 | 5282682 | Gold Hammer | silica-pyrite alteration | Muscovite,Pyrophyllite | 75.68 | 14.19 | 2.29 | - | - | 0.002 | 0.03 | 0.01 | 0.14 | 2.50 | 0.503 |
| GS-11-373 | 658700 | 5282715 | Gold Hammer | white mica-pyrite alteration | Muscovite | 57.00 | 15.93 | 11.47 | 6.40 | 4.56 | 0.040 | 1.36 | 0.27 | - | 4.21 | 1.737 |
| GS-11-375 | 658690 | 5282775 | Gold Hammer | silica-pyrite alteration | Pyrophyllite | 88.61 | 7.88 | 1.19 | 0.07 | 1.01 | - | - | - | - | 0.10 | 0.583 |
| GS-11-378 | 658832 | 5282916 | Gold Hammer | white mica-silica alteration | FeChlorite,Paragonite | 85.47 | 7.12 | 2.90 | - | - | 0.008 | 0.03 | - | - | 1.40 | 0.164 |
| GS-11-390 | 658368 | 5282630 | Gold Hammer | silica-pyrite alteration | Muscovite,Pyrophyllite | 83.32 | 9.56 | 1.53 | - | - | 0.001 | - | - | - | 1.37 | 0.175 |
| GS-11-395 | 658887 | 5282387 | Gold Hammer | beige silica alteration | Paragonite | 88.51 | 7.04 | 1.63 | 0.13 | 1.35 | 0.004 | - | - | - | 1.84 | 0.143 |
| GS-11-396 | 658887 | 5282387 | Gold Hammer | hematite-rich breccia | Muscovite | 79.19 | 4.32 | 13.37 | 13.04 | 0.30 | 0.012 | - | - | - | 1.33 | 0.185 |
| GS-11-399 | 658986 | 5282989 | Gold Hammer | beige silica alteration | Muscovite | 79.51 | 11.71 | 1.94 | - | - | 0.016 | 0.06 | 0.01 | 0.88 | 4.07 | 0.188 |
| GS-11-403 | 658844 | 5283067 | Gold Hammer | beige silica alteration | Muscovite | 85.59 | 7.68 | 1.39 | 0.92 | 0.42 | 0.011 | 0.05 | - | - | 2.52 | 0.164 |
| GS-11-407 | 659152 | 5283302 | Gold Hammer | silica-pyrite alteration | Phengitic Illite | 76.91 | 11.04 | 3.04 | - | - | 0.035 | 0.02 | 0.03 | 1.39 | 4.90 | 0.172 |
| GS-11-409 | 659062 | 5283144 | Gold Hammer | silica-pyrite alteration | Muscovite | 79.01 | 11.25 | 2.25 | 1.37 | 0.79 | 0.011 | 0.04 | - | - | 3.86 | 0.184 |
| GS-11-441 | 659195 | 5283204 | Gold Hammer | felsic volcanic crosscut by K-feldspar-rich veinlets | | 63.46 | 17.50 | 5.28 | 2.12 | 2.84 | 0.079 | 0.20 | 0.07 | 6.89 | 3.85 | 0.300 |
| GS-11-442 | 659189 | 5283212 | Gold Hammer | hematitic volcaniclastic | Montmorillonite | 64.10 | 16.03 | 5.17 | 2.50 | 2.40 | 0.098 | 0.20 | 0.46 | 5.85 | 4.57 | 0.459 |
| GS-11-444 | 659202 | 5283377 | Gold Hammer | silica-pyrite alteration | Muscovite | 79.72 | 10.86 | 2.21 | 0.74 | 1.32 | 0.023 | - | - | - | 5.14 | 0.180 |
| GS-11-446 | 659280 | 5283535 | Gold Hammer | silica-pyrite alteration crosscut by cm-scale quartz veins | Phengite | 64.57 | 8.50 | 12.52 | 4.41 | 7.30 | 0.064 | 0.39 | 0.09 | - | 2.91 | 2.090 |
| GS-11-447 | 659289 | 5283507 | Gold Hammer | beige chalcedonic silica veining | Phengite | 85.43 | 7.39 | 1.19 | 0.89 | 0.27 | 0.012 | 0.23 | 0.01 | - | 2.95 | 0.186 |
| GS-11-449 | 659292 | 5283505 | Gold Hammer | weakly banded chalcedonic silica veining | Phengite | 82.90 | 8.03 | 1.07 | 0.67 | 0.36 | 0.011 | 0.17 | 0.02 | - | 4.82 | 0.179 |
| GS-11-451 | 659280 | 5283488 | Gold Hammer | beige chalcedonic silica veining | Phengite | 90.05 | 5.57 | 1.54 | 1.48 | 0.05 | 0.014 | 0.11 | 0.01 | - | 2.43 | 0.111 |
| GS-11-452 | 659278 | 5283487 | Gold Hammer | weakly banded chalcedonic silica veining | Phengite | 82.80 | 7.96 | 1.21 | 0.79 | 0.38 | 0.010 | 0.16 | 0.02 | - | 4.15 | 0.187 |
| GS-12-233 | 659289 | 5283507 | Gold Hammer | beige chalcedonic silica veining | Phengite | N/A | N/A | N/A | N/A | N/A | N/A | N/A | N/A | N/A | N/A | N/A |
| GS-12-234 | 659289 | 5283507 | Gold Hammer | beige chalcedonic silica veining | Phengite | N/A | N/A | N/A | N/A | N/A | N/A | N/A | N/A | N/A | N/A | N/A |
| GS-12-235 | 659289 | 5283507 | Gold Hammer | beige chalcedonic silica veining | Phengite | N/A | N/A | N/A | N/A | N/A | N/A | N/A | N/A | N/A | N/A | N/A |
| GS-12-236 | 658227 | 5283305 | Gold Hammer | silicified volcaniclastic | | N/A | N/A | N/A | N/A | N/A | N/A | N/A | N/A | N/A | N/A | N/A |
| GS-12-237 | 658244 | 5283278 | Gold Hammer | silica-pyrite alteration | Muscovite | N/A | N/A | N/A | N/A | N/A | N/A | N/A | N/A | N/A | N/A | N/A |
| GS-12-238 | 658259 | 5283240 | Gold Hammer | beige silica alteration | | N/A | N/A | N/A | N/A | N/A | N/A | N/A | N/A | N/A | N/A | N/A |
| GS-12-242 | 658075 | 5283539 | Gold Hammer | grey silica-pyrite alteration with up to 20% pyrite | Muscovite | N/A | N/A | N/A | N/A | N/A | N/A | N/A | N/A | N/A | N/A | N/A |
| GS-12-244 | 658089 | 5283537 | Gold Hammer | beige silica alteration | Muscovite | 97.73 | 0.45 | 0.09 | - | - | - | - | 0.02 | - | 0.10 | 0.163 |
| GS-11-455 | 699307 | 5295047 | Hickey's Pond | silica-alunite alteration; no pyrite | Na Alunite | 62.76 | 13.54 | 0.37 | 0.26 | 0.10 | 0.001 | - | 0.06 | 0.90 | 2.23 | 0.522 |
| GS-11-456 | 699320 | 5295031 | Hickey's Pond | alunite-specularite alteration | Na Alunite | 56.87 | 14.57 | 2.07 | 2.04 | 0.03 | 0.001 | - | 0.05 | 1.23 | 2.08 | 0.589 |
| GS-11-457 | 699316 | 5295025 | Hickey's Pond | vuggy silica zone | | 87.69 | 2.15 | 4.01 | 3.76 | 0.23 | 0.003 | - | 0.02 | 0.04 | 0.17 | 0.424 |
| GS-11-460 | 699326 | 5295013 | Hickey's Pond | silica-specularite-alunite alteration | Na Alunite | 64.67 | 11.18 | 3.90 | 2.09 | 1.63 | 0.003 | 0.01 | 0.05 | 1.23 | 1.22 | 0.756 |
| GS-11-461 | 699428 | 5294996 | Hickey's Pond | alunite-specularite alteration | Na Alunite | 62.57 | 12.91 | 3.85 | 3.80 | 0.05 | 0.003 | - | 0.10 | 0.79 | 2.33 | 0.522 |

**Table 1.** *(Continued)* Geochemical samples collected in relation to mapping of select zones of advanced argillic alteration; also included are representative samples from the Hickey's Pond prospect for comparison. Note: N/A = not analyzed; - = below detection limit; coordinates are listed in NAD27, Zone 21

| Sample | P2O5 | LOI | Au | Ag | As | Ba | Be | Bi | Cd | Cr | Cu | Hg | Mo | P | Pb | S | Sb | Se | Sn | Te | Tl | W | Zn |
|---|---|---|---|---|---|---|---|---|---|---|---|---|---|---|---|---|---|---|---|---|---|---|---|
| | % | % | ppb | ppm | ppm | ppm | ppm | ppm | ppm | ppm | ppm | ppm | ppm | ppm | % | ppm | ppm | ppm | ppm | ppm | ppm | ppm | |
| | 0.001 | 0.01 | 5 | 0.2 | 2 | 1 | 0.1 | 0.1 | 0.1 | 1 | 1 | 1 | 1 | 1 | 1 | 0.01 | 0.1 | 0.1 | 1 | 0.1 | 0.01 | 1 | 1 |
| GS-11-02 | 0.019 | 2.37 | - | - | - | 373 | 1.2 | 1.4 | 0.2 | 3 | 10 | - | 14 | 81 | 32 | 1.02 | 0.6 | 2.1 | 6 | 0.4 | 1.11 | 2 | 32 |
| GS-11-03 | 0.253 | 4.43 | - | N/A | 7 | 224 | 1.2 | - | 0.1 | 1 | 11 | N/A | 1 | 1040 | 4 | N/A | 1.2 | - | 2 | N/A | - | - | 79 |
| GS-11-04 | 0.055 | 0.56 | - | - | 5 | 349 | 0.1 | 0.2 | - | 2 | 2 | - | - | 253 | 43 | 0.04 | 4.6 | - | - | 0.5 | - | 4 | 4 |
| GS-11-05 | 0.095 | 0.43 | - | - | 3 | 153 | 0.2 | 1.2 | - | 2 | 3 | - | - | 445 | 12 | - | 3.5 | - | - | 0.3 | - | 3 | 3 |
| GS-11-10 | 0.199 | 12.34 | 5 | - | 16 | 446 | 0.2 | 0.7 | - | 2 | 4 | - | 9 | 778 | 19 | 4.05 | 1.7 | 4.9 | - | 2.1 | 0.24 | 2 | 2 |
| GS-11-11 | 0.222 | 8.53 | - | - | 4 | 614 | - | 0.8 | - | 2 | - | - | 3 | 907 | 17 | 2.57 | 3.0 | 0.6 | - | 0.4 | 0.09 | 1 | 2 |
| GS-11-13 | 0.185 | 3.31 | - | N/A | 6 | 85 | 1.4 | - | 0.1 | 1 | 13 | N/A | 1 | 765 | 4 | N/A | 1.0 | - | 2 | N/A | - | 3 | 75 |
| GS-11-84 | 0.167 | 4.37 | - | N/A | 10 | 911 | 1.9 | - | - | 5 | 3 | N/A | 1 | 680 | 11 | N/A | 0.6 | - | 5 | N/A | - | 2 | 66 |
| GS-11-86 | 0.166 | 19.57 | 30 | - | 10 | 746 | 0.1 | 0.78 | - | 1 | 2 | - | - | 702 | 6 | 0.97 | 5.2 | 0.9 | 5 | 0.4 | - | 2 | 2 |
| GS-11-87 | 0.194 | 5.90 | - | N/A | 13 | 697 | 1.9 | - | - | 18 | 49 | N/A | 1 | 768 | 13 | N/A | 1.1 | 2.0 | 3 | N/A | - | 1 | 115 |
| GS-11-112 | 0.093 | 4.51 | 32 | - | 24 | 462 | 1.7 | 2.1 | - | 1 | 14 | - | 3 | 388 | 41 | 0.21 | 1.7 | 1.8 | 4 | 0.3 | 1.01 | 2 | 48 |
| GS-11-114 | 0.141 | 1.97 | - | N/A | 5 | 16 | 1.8 | - | 0.2 | 42 | 5 | N/A | - | 600 | 15 | N/A | 1.1 | - | 4 | N/A | - | 2 | 81 |
| GS-11-115 | 0.015 | 1.36 | - | N/A | 2 | 274 | 3.3 | - | - | 3 | 1 | N/A | 2 | 74 | 8 | N/A | 0.6 | - | 6 | N/A | - | - | 20 |
| GS-11-125 | 0.175 | 6.50 | - | N/A | 26 | 245 | 1.2 | - | 0.1 | 76 | 54 | N/A | - | 670 | 2 | N/A | 2.1 | 5.0 | 2 | N/A | - | - | 75 |
| GS-11-126 | 0.133 | 21.33 | - | - | 7 | 864 | 0.3 | 0.2 | - | 3 | 3 | - | 2 | 575 | 41 | 7.79 | 0.8 | 0.4 | 2 | 0.3 | 0.09 | 2 | 2 |
| GS-11-127 | 0.183 | 14.85 | 11 | - | 12 | 814 | 0.2 | 3.1 | - | 3 | 6 | - | 1 | 748 | 118 | 4.66 | 5.5 | 2.0 | 2 | 0.6 | 0.31 | 2 | 2 |
| GS-11-466 | 0.066 | 3.55 | 54 | - | 11 | 277 | - | 11.3 | - | 2 | 2 | - | - | 303 | 27 | 0.35 | 9.8 | 1.6 | 3 | 4.2 | 0.29 | 3 | - |
| GS-11-470 | - | 1.46 | - | 0.3 | 2 | 110 | 5.0 | 0.4 | 3.0 | - | 153 | - | - | 20 | 401 | 1.01 | 0.4 | 4.6 | 5 | 0.6 | - | 1 | 219 |
| GS-11-134 | 0.223 | 7.49 | - | - | 6 | 539 | 0.5 | 2.5 | - | 3 | 14 | - | 9 | 701 | 42 | 2.24 | 1.8 | 8.4 | 2 | 2.0 | 0.34 | 5 | 14 |
| GS-11-136 | 0.161 | 17.85 | - | - | 2 | 853 | 0.2 | 0.2 | - | 4 | 2 | - | 2 | 679 | 155 | 6.38 | 1.5 | - | 7 | - | 0.07 | 30 | 3 |
| GS-11-138A | 0.116 | 15.62 | 10 | N/A | 4 | 413 | 0.1 | - | - | 3 | 43 | N/A | 36 | 492 | 37 | N/A | 0.6 | 9.0 | 2 | N/A | - | 16 | 6 |
| GS-11-138B | 0.117 | 14.27 | - | N/A | - | 445 | 0.1 | - | - | 3 | 3 | N/A | 1 | 496 | 34 | N/A | 0.6 | - | 2 | N/A | - | 16 | 5 |
| GS-11-139 | 0.164 | 12.49 | - | - | 3 | 859 | - | 0.9 | - | 3 | 2 | - | 3 | 656 | 228 | 3.71 | 1.3 | - | 5 | - | - | 20 | 2 |
| GS-11-140 | 0.335 | 23.97 | - | N/A | 3 | 1608 | 0.2 | - | - | 5 | 1 | N/A | 5 | 1217 | 354 | N/A | 1.0 | - | 10 | N/A | - | 25 | 6 |
| GS-11-144 | 0.165 | 12.49 | 50 | - | 7 | 854 | 0.1 | 4 | - | 5 | 15 | - | 27 | 649 | 477 | 5.84 | 0.7 | 2.6 | 17 | 0.6 | 0.08 | 5 | 4 |
| GS-11-145 | 0.145 | 16.72 | 76 | - | 13 | 1026 | - | 1.4 | - | 2 | 12 | - | 99 | 232 | 196 | 1.63 | 1.2 | 1.7 | 25 | 0.4 | 0.07 | 10 | 8 |
| GS-11-147 | 0.432 | 3.28 | - | - | 3 | 191 | 0.6 | 0.9 | - | - | 2 | - | 2 | 657 | 28 | 0.24 | 3.4 | 0.2 | 1 | - | 1.15 | 6 | 27 |
| GS-11-154 | 0.212 | 1.91 | - | N/A | - | 546 | 1.0 | - | 0.2 | 1 | 2 | N/A | - | 898 | 7 | N/A | 0.3 | - | 1 | N/A | - | 1 | 83 |
| GS-12-29 | N/A | N/A | - | - | - | 25 | 1.7 | - | - | N/A | 6 | - | - | N/A | 9 | 2.02 | 0.9 | 2.8 | N/A | 1.5 | - | - | 7 |
| GS-12-88 | 0.110 | 2.76 | - | - | - | 551 | 1.9 | - | | 4 | 8 | N/A | 18 | N/A | 18 | N/A | 0.3 | - | 3 | N/A | - | 4 | 75 |
| GS-12-89 | N/A | N/A | 21 | 0.5 | 3 | 31 | 0.2 | 1.31 | - | N/A | 21 | - | 16 | N/A | 4 | 3.35 | 2.1 | 33.5 | N/A | 0.4 | - | - | 3 |
| GS-12-221 | N/A | N/A | - | - | 5 | 50 | 1.5 | - | - | N/A | 5 | - | - | N/A | 12 | 1.56 | 0.6 | 2.9 | N/A | 1.3 | - | - | 13 |
| GS-11-359 | 0.020 | 1.51 | - | N/A | 39 | 30 | 0.8 | - | - | 2 | 1 | N/A | 4 | 56 | 5 | N/A | 5.0 | - | 10 | N/A | 0.14 | 7 | 10 |
| GS-11-362 | - | 0.56 | - | N/A | 5 | 20 | 2.9 | - | - | 2 | 4 | N/A | - | 16 | 6 | N/A | 1.2 | - | 9 | N/A | - | 2 | 86 |
| GS-11-364 | 0.003 | 0.78 | 16 | 0.4 | 86 | 28 | 0.6 | 0.47 | - | 3 | 4 | - | 31 | 20 | 11 | 0.22 | 6.2 | 0.3 | 12 | 0.4 | - | 5 | 2 |
| GS-11-365 | 0.050 | 2.98 | - | N/A | 80 | 123 | 2.3 | - | 0.5 | 9 | 6 | N/A | 13 | 164 | 29 | N/A | 3.9 | - | 11 | N/A | - | 5 | 48 |
| GS-11-373 | 0.265 | 7.09 | - | - | 17 | 253 | 5.0 | 0.17 | 0.7 | 177 | 45 | - | 1 | 1151 | 27 | 6.21 | 3.4 | 1.1 | 6 | 0.1 | 0.53 | 3 | 159 |
| GS-11-375 | 0.047 | 2.21 | 33 | 0.2 | 143 | 17 | 0.9 | 1.01 | - | 8 | 3 | - | 18 | 168 | 29 | 0.81 | 5.9 | 5.1 | 17 | 0.1 | 0.97 | 12 | 8 |
| GS-11-378 | 0.001 | 1.46 | - | - | 9 | 18 | 0.9 | - | - | 2 | 3 | - | 2 | 12 | 30 | 0.15 | 1.0 | 0.8 | 6 | - | 0.65 | 3 | 71 |
| GS-11-390 | 0.002 | 2.38 | - | - | 63 | 38 | 1.2 | - | - | 1 | 2 | - | 1 | 18 | 9 | 1.15 | 6.1 | 0.3 | 7 | 0.1 | 0.48 | 3 | 3 |
| GS-11-395 | 0.003 | 1.59 | - | - | 41 | 20 | 0.6 | 0.17 | - | 1 | 3 | - | 11 | 13 | 9 | 0.50 | 5.9 | 0.4 | 9 | - | 0.22 | 5 | 11 |
| GS-11-396 | 0.017 | 0.93 | - | 0.2 | 100 | 18 | 1.7 | 0.4 | 0.9 | 1 | 3 | - | 1 | 69 | 41 | 0.00 | 23.8 | 0.3 | 13 | - | 0.12 | 23 | 32 |
| GS-11-399 | 0.002 | 1.75 | - | - | 32 | 43 | 3.6 | - | - | 1 | 3 | - | 12 | 13 | 16 | 0.49 | 0.9 | 0.6 | 10 | - | - | 1 | 87 |
| GS-11-403 | 0.007 | 1.34 | - | - | 14 | 15 | 1.9 | 0.5 | - | 3 | 5 | - | 23 | 49 | 22 | 0.01 | 1.9 | 0.5 | 6 | - | - | 2 | 7 |
| GS-11-407 | 0.002 | 1.37 | - | N/A | 7 | 35 | 4.2 | - | 0.6 | 2 | 3 | N/A | - | 12 | 17 | N/A | 0.5 | - | 9 | N/A | 0.62 | 2 | 174 |
| GS-11-409 | - | 1.92 | - | - | 12 | 11 | 2.5 | - | - | - | - | - | 2 | 15 | 6 | 0.02 | 0.9 | 0.3 | 11 | - | - | 3 | 8 |
| GS-11-441 | 0.041 | 0.93 | - | N/A | 3 | 52 | 3.5 | - | - | 2 | 4 | N/A | 2 | 193 | - | N/A | 0.4 | - | 6 | N/A | 0.22 | 3 | 127 |
| GS-11-442 | 0.098 | 1.02 | - | N/A | 5 | 51 | 2.9 | - | - | 3 | 7 | N/A | 3 | 448 | - | N/A | 0.4 | - | 7 | N/A | 0.16 | 3 | 141 |
| GS-11-444 | - | 1.96 | 28 | - | 69 | 61 | 1.9 | 0.1 | 0.7 | 1 | 4 | - | 2 | 17 | 194 | 0.76 | 0.9 | 1.3 | 10 | - | - | 2 | 144 |
| GS-11-446 | 0.089 | 7.29 | 22 | N/A | 690 | 53 | 5.2 | - | 1.5 | 86 | 48 | N/A | 40 | 395 | 13 | N/A | 3.4 | 22.0 | 2 | N/A | 0.10 | 5 | 256 |
| GS-11-447 | 0.013 | 1.41 | - | - | 19 | 145 | 3.0 | 0.21 | - | 2 | 3 | - | 8 | 63 | 31 | 0.03 | 2.6 | 1.5 | 3 | 0.2 | - | 1 | 9 |
| GS-11-449 | 0.012 | 1.06 | 10 | - | 25 | 268 | 2.3 | 0.27 | - | 2 | 4 | - | 6 | 60 | 31 | 0.02 | 2.0 | 0.7 | 3 | 0.2 | - | 1 | 10 |
| GS-11-451 | 0.028 | 1.06 | 27 | - | 44 | 119 | 2.3 | 0.2 | - | 2 | 3 | - | 6 | 126 | 115 | 0.02 | 3.4 | 2.1 | 3 | - | 0.50 | 3 | 17 |
| GS-11-452 | 0.016 | 1.12 | 113 | - | 21 | 225 | 2.8 | 0.26 | - | 2 | 2 | - | 5 | 83 | 61 | 0.01 | 2.4 | 1.6 | 3 | 0.1 | 0.19 | 2 | 11 |
| GS-12-233 | N/A | N/A | - | - | 14 | 15 | 3.2 | 0.37 | - | N/A | 5 | - | - | N/A | 14 | 0.02 | 0.9 | 0.7 | N/A | 0.5 | 0.10 | - | 7 |
| GS-12-234 | N/A | N/A | - | - | 27 | 15 | 2.7 | 0.19 | - | N/A | 27 | - | 2 | N/A | 69 | 0.05 | 1.3 | 0.8 | N/A | 0.3 | - | - | 47 |
| GS-12-235 | N/A | N/A | 26 | - | 22 | 16 | 2.6 | 0.17 | - | N/A | 4 | - | 4 | N/A | 87 | 0.03 | 1.1 | 1.0 | N/A | 0.4 | 0.10 | - | 15 |
| GS-12-236 | N/A | N/A | - | - | 7 | 8 | 0.3 | - | - | N/A | - | - | 10 | N/A | 14 | 0.00 | 1.0 | 0.1 | N/A | 0.2 | - | 9 | 7 |
| GS-12-237 | N/A | N/A | - | 0.2 | 38 | 8 | 2.1 | - | - | N/A | 3 | - | - | N/A | 21 | 0.06 | 1.0 | 0.6 | N/A | 0.2 | - | - | 10 |
| GS-12-238 | N/A | N/A | - | - | 35 | 5 | 0.8 | 0.3 | - | N/A | - | - | 14 | N/A | 24 | 0.42 | 3.9 | - | N/A | 0.4 | - | 44 | 24 |
| GS-12-242 | N/A | N/A | - | 1.3 | 53 | 6 | 0.7 | 0.42 | 0.9 | N/A | 34 | 7 | 49 | N/A | 148 | 7.91 | 2.4 | 3.2 | N/A | 0.3 | 0.60 | - | 111 |
| GS-12-244 | 0.006 | 0.36 | - | 0.4 | - | 4 | 0.4 | 0.1 | - | 5 | 3 | - | 3 | N/A | 27 | 0.01 | 0.3 | - | 6 | 0.3 | - | 1 | 5 |
| GS-11-455 | 0.159 | 16.45 | 632 | 0.2 | 18 | 571 | - | 5.28 | - | 6 | 4 | - | 2 | 737 | 76 | 1.08 | 12.2 | 7.3 | 6 | 3.7 | - | 6 | 2 |
| GS-11-456 | 0.162 | 17.85 | 143 | - | 5 | 727 | - | 2.11 | - | 5 | 4 | - | - | 731 | 58 | 1.14 | 21.8 | 0.5 | 4 | 1.1 | - | 2 | 2 |
| GS-11-457 | 0.054 | 4.40 | 31000 | 110 | 2830 | 140 | - | 476 | - | 4 | 336 | 27 | 5 | 208 | 31 | 0.56 | 2690.0 | 139.0 | 851 | 789.0 | - | 1 | 4 |
| GS-11-460 | 0.122 | 15.66 | 179 | 0.6 | 10 | 470 | - | 4.78 | - | 37 | 24 | - | - | 514 | 46 | 3.49 | 15.0 | 11.0 | 6 | 10.8 | - | - | 2 |
| GS-11-461 | 0.217 | 15.82 | 6 | 0.3 | 6 | 717 | - | 0.26 | - | 4 | 3 | - | 1 | 900 | 147 | 0.69 | 1.6 | 0.2 | 2 | 0.2 | - | 2 | 7 |

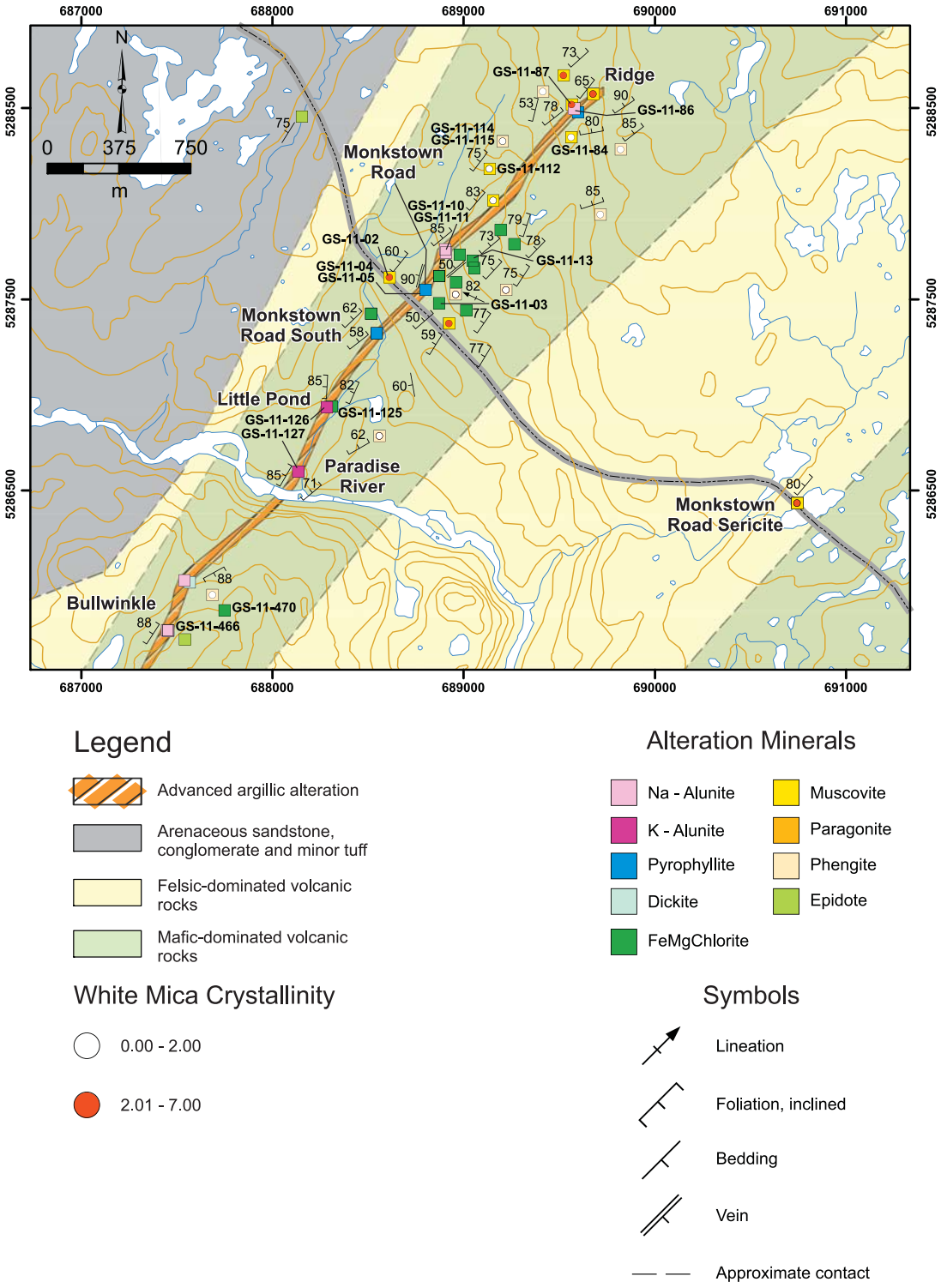


**Figure 4.** *Regional geology map outlining the distribution of the advanced argillic alteration along the Monkstown Road Belt as well as the location of the various prospects. Also shown are the sample locations with their corresponding dominant mineral phase as determined by VIRS, along with the white mica crystallinity of the various white mica phases; red dots denote high temperature phases based on WMC indexing. Labelled samples correspond to geochemical analyses in Table 1. Note the alteration zone extends beyond the limits of the map to the southwest toward the Strange prospect.*

**Plate 2.** *Strongly foliated and crenulated muscovite alteration exposed along Monkstown Road, located immediately west of the Monkstown Road prospect. Samples of the alteration have WMC index of 3.5, indicating a high temperature of formation. This style of alteration is often accompanied by abundant pyrite and is generally barren with respect to gold mineralization.*

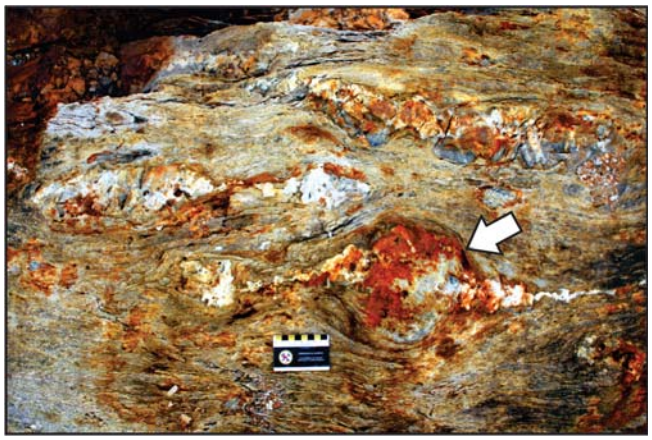

**Plate 3.** *Boudinaged lens of silica alteration (arrow) hosted within alunite–specularite alteration demonstrating the high degree of deformation developed within the advanced argillic alteration.*


**Plate 4.** *Photograph showing the pale purple alunite–specularite–pyrophyllite alteration being overprinted by a secondary alunite–pyrite assemblage, Tower prospect; inset shows a cut sample of the contact showing the location of the respective VIRS analyses.*

prospect (Huard and O'Driscoll, 1986). The Tower prospect occurs approximately 11 km to the southwest of, and roughly along strike from the Hickey's Pond prospect, which is host to high-grade gold mineralization in association with vuggy silica and advanced argillic alteration (O'Brien *et al.,* 1999; Figure 3). The Tower prospect was first discovered by Huard and O'Driscoll (1986) and, like the Monkstown Road Belt, the alteration zone has been the subject of intermittent mineral exploration (*e.g.,* Reusch, 1985; McBride, 1987; Hayes, 2000; Dimmell, 2003; Dyke and Pratt, 2008). Assay results from this exploration have identified weakly anomalous gold and molybdenum values in association with the advanced argillic alteration (up to 179 ppb Au and up to 203 ppm Mo; Dimmell, 2003). Exploration trenching in the area by Cornerstone Resources in 2007 indicates that the alteration zone is up to 150–200 m wide, and hosts weak zones of hydrothermal brecciation. The best assay value reported from channel sampling of the alteration zone was 62.4 ppb Au over 3.0 m (Dyke and Pratt, 2008).

Spectroscopic investigations of alteration by Dyke and Pratt (2008) noted the presence of alunite, pyrophyllite, muscovite and illite with lesser topaz. Large lenses of boudinaged silica alteration were also noted and mapped in the zone during trenching (Plate 3). Locally, some of these lenses display a vuggy texture, but they do not contain gold mineralization. Sampling conducted as part of this study confirmed the presence of topaz, which is locally developed with silica alteration similar to that observed within the boudinaged lenses; the presence of topaz indicates relatively high temperatures of formation (>260° C, Reyes, 1990). Spectral results of alunite alteration from the area confirm the presence of sodic alunite throughout the alteration zone. The trenching also exposed evidence of at least two stages of fluid alteration associated with the advanced argillic alteration. Pervasive sodic alunite–specularite–pyrophyllite alteration is locally overprinted by a secondary patchy alteration consisting of sodic alunite–pyrite (Plate 4). This latter alteration is associated with anomalous Au, Cu, Mo and Se relative to the sodic alunite–specularite–pyrophyllite alteration (GS-11-138A and B, Table 1). During mapping of the alteration, large angular blocks containing sodic alunite–pyrite alteration were found along strike of the main Tower prospect along the shoreline of a pond, and are interpreted as subcrop. These blocks are similarly anomalous in Au, Cu, Mo and Se (GS-12-89, Table 1).

The advanced argillic alteration zone is inferred to be bounded both to the east and west by fault structures. These structures are apparent as two roughly subparallel linear conductive zones near the central portion of a VLF survey conducted by Hayes (2000). The western structural contact is locally exposed along the western shoreline of a pond to the southwest of the alteration zone (Figure 5). Here, strongly foliated and folded muscovite–pyrite alteration (Plate 5) marks the western limit of the hydrothermal alteration. Samples having a strong muscovite alteration are structurally controlled, aside from some samples adjacent to an intrusion located to the immediate northwest of the alteration, which are related to contact metamorphism (Figure 5). The muscovite alteration is characterized by a WMC of >2. Outside of the main alteration zone, the felsic volcanic rocks are dominated by phengite alteration, which also displays a WMC of >2, but is interpreted to be a regional signature. It does not appear that WMC alone is useful in defining zones of hydrothermal alteration at the Tower prospect.

Northwest of the Tower prospect, an intrusion of granodiorite is exposed, which corresponds with magnetic highs as defined by a geophysical survey conducted by Hayes (2000), and the outline of the unit is drawn in Figure 5 to correspond with the magnetic highs in this area. Detailed mapping suggests that the intrusive rocks are less extensive than suggested by the regional map of Huard and O'Driscoll (1986). A sample of felsic volcanic rock collected in this area for geochronological study (GS-11-428; Figure 5; *see* below), from within a sequence locally exhibiting a fragmental texture (Plate 6) provides supporting evidence for an extrusive origin of the volcanic rocks.

## GOLD HAMMER PROSPECT

Pyrophyllite–diaspore advanced argillic alteration associated with the Gold Hammer prospect (Figure 1; Hussey, 2009), represents the first example of this style of alteration identified within the volcanic rocks of the Long Harbour Group. The alteration zone is developed on the southeastern limb of the southwest-plunging Femme Syncline of O'Brien *et al*. (1984). The alteration is developed close to the contact between the *ca.* 570 Ma Belle Bay Formation and the overlying *ca.* 550 Ma Mooring Cove Formation (O'Brien *et al*., 1984, 1994).

The Gold Hammer prospect contains up to 61 g/t Au (Hussey, 2006) associated with stockwork-style chalcedonic silica veins and marginal phengite alteration of the wall rock. Sampling of the area identified anomalous gold (113 ppb), and a zone of pyritic alteration immediately adjacent to the main zone of chalcedonic silica veining has highly anomalous As and Se, and weakly anomalous Cu, Mo and Zn (GS-11-446; Table 1).

Approximately 850 m to the southwest of the Gold Hammer prospect, field mapping outlined a zone of pyrophyllite–diaspore-rich advanced argillic alteration that can be traced intermittently for more than of 1.5 km along strike (Figure 6). Such alteration is indicative of paleotemperatures >200°C (Reyes, 1990). This alteration is developed within flow-banded rhyolite and related volcaniclastic sedimentary rocks. Locally, what is inferred to have been a fragmental volcanic unit contains 10- to 15-cm-scale relic fragments (now altered to diaspore) supported within a pyrophyllite-rich matrix (Plate 7). A prominent northeast-trending linear containing variably developed muscovite alteration, characterized by a WMC of >3, links the zone of advanced argillic alteration to the Gold Hammer prospect and may have been a fluid conduit. From the main occurrence of pyrophyllite–diaspore alteration the advanced argillic alteration extends westward and is largely stratiform in its distribution. The eastern portion of the advanced argillic alteration is stratigraphically overlain by a muscovite–pyrite-altered tuff-breccia, which is locally host to angular fragments of silica alteration of a possible hydrothermal origin (Plate 8). This clast may provide evidence for erosion of the underlying hydrothermal system.

Farther west, the alteration is developed subparallel to the contact between the host felsic volcanic rocks and the overlying siliciclastic sedimentary rocks and related mafic flows. These latter rocks are unaffected by the underlying advanced argillic alteration, which suggests one of two possibilities: either 1) the overlying rocks were impermeable to the hydrothermal fluids or, 2) the siliciclastic sedimentary rocks and related mafic flows postdate the development of the underlying hydrothermal alteration. The local development of muscovite alteration, within what appear to be relatively unaltered siliciclastic sedimentary rocks, is inferred to be related to contact metamorphism as indicated by the local development of hornfels close to the contact with the overlying mafic flows, rather than being related to the underlying advanced argillic alteration (Figure 6). Localized zones of intense silica ± pyrite alteration hosting anomalous values of As, Se, Cu and Mo (GS-12-242; Table 1) are developed within a volcaniclastic unit to the north of the main alteration zone. The silica alteration again displays a largely stratiform distribution formed proximal to a prominent northeast-trending structure (Figure 6).

Outside the advanced argillic alteration zone, country rocks are dominated by purple flow-banded rhyolite, which displays regional phengite and muscovite alteration characterized by a WMC of <3. To the northeast of the map area, the Long Harbour Group is intruded by a composite suite of alkaline gabbro, granodiorite and biotite granite along with lesser peralkaline granite and syenite, known as the Cross Hills Intrusive Suite (Tuach, 1991; Figure 1). The intrusion

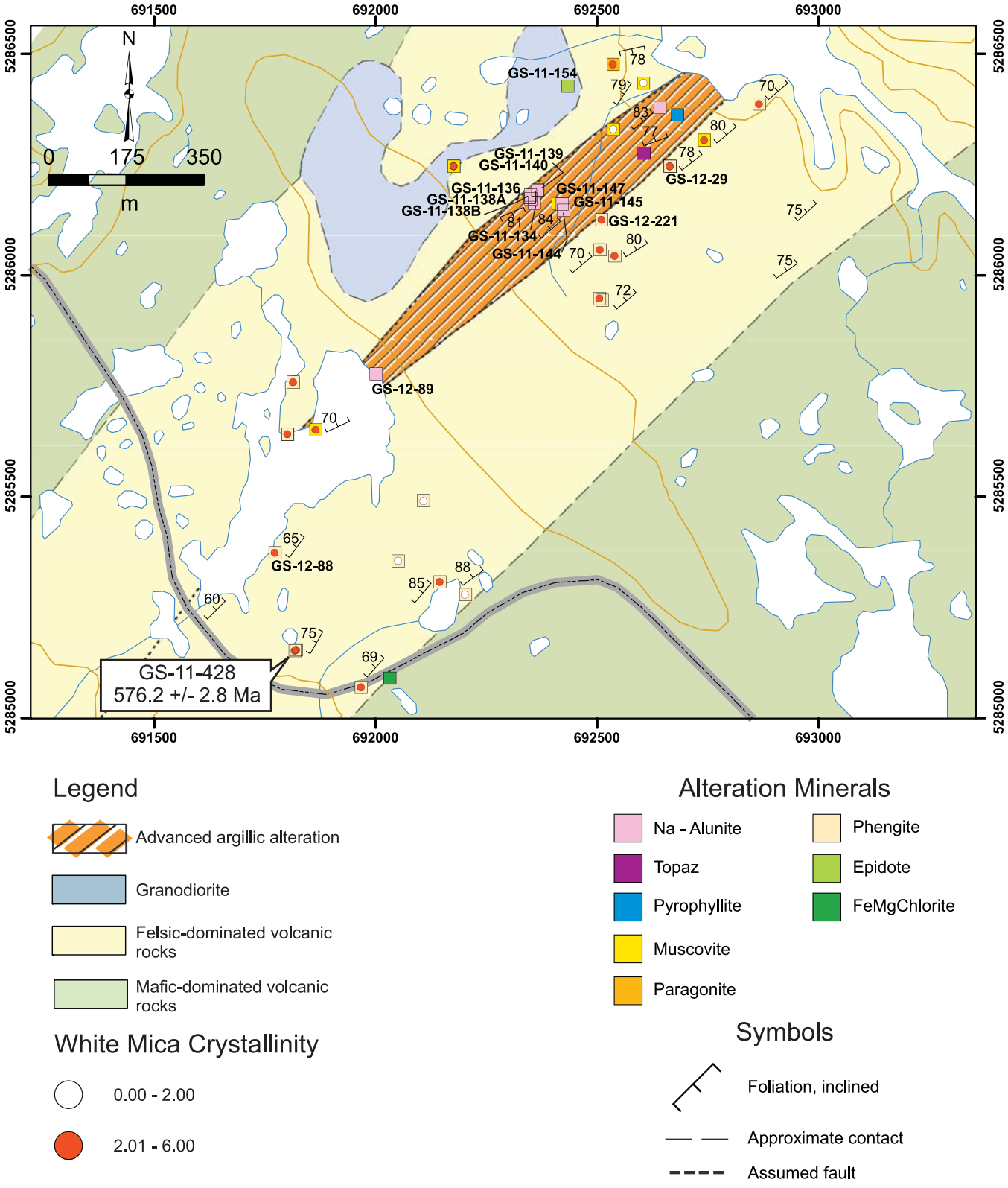


**Figure 5.** *Regional geology map outlining the distribution of the advanced argillic alteration at the Tower prospect (base-map geology modified from Huard and O'Driscoll, 1986). Also shown are the sample locations with their corresponding dominant mineral phase as determined by VIRS along with the white mica crystallinity of the various white mica phases (refer to text for discussion of results). Labelled samples correspond to geochemical analyses in Table 1.*

**Plate 5.** *Strongly foliated and crenulated muscovite–pyrite alteration that marks the western limit of the hydrothermal alteration developed at the Tower prospect.*


**Plate 6.** *Locally preserved fragmental volcanic rock that is interbedded with the fine-grained felsic tuff sampled for geochronological study.*

of the Cross Hills Intrusive Suite is associated with the development of extensive zones of pyritic alteration (O'Brien *et al*., 1984), and represents a potential heat source for the development of the advanced argillic alteration within the Long Harbour Group. On a regional scale, a sample of the Cross Hills Intrusive Suite was collected to try and better constrain its age, relative to that of the volcanic rocks hosting the advanced argillic alteration (*see* below).

## DISCOVERIES OF NEW EPITHERMAL ALTERATION ZONES

This study has identified several new alteration zones, some of which contain associated geochemical anomalies suggestive of an epithermal origin. Other alteration zones, which were previously known but poorly documented, have been confirmed to represent zones of advanced argillic alteration. The following section of the report provides a brief summary these zones.

### RATTLE BROOK

The Rattle Brook occurrence represents a previously known zone of advanced argillic alteration that has received cursory exploration work in the form of trenching; however, this work has not been reported. The Rattle Brook occurrence is located immediately northwest of the Burin Highway near its intersection with Rattle Brook (Figure 1). The prospect has several exploration trenches spread over a strike length of approximately 1 km. These trenches expose intense silicification, locally displaying well-developed cataclastic brecciation, along with associated advanced argillic alteration hosted within felsic volcanic rocks of the Marystown Group. The roughly east–west-trending alteration can be traced, intermittently, along Rattle Brook both upstream and downstream from the Burin Highway, with known alteration extending, intermittently, along strike for upward of 2.3 km. The alteration appears to be structurally truncated at both its eastern and western limits. Throughout its strike length, the alteration is characterized by pyrophyllite, dickite, alunite, muscovite and pyrite assemblages, associated with intense silicification. Geochemical sampling at the eastern extent of the alteration zone identified weakly anomalous gold values (27 ppb) in association with strong pyritic alteration (GS-12-150; Table 2). Along strike to the northeast of the inferred eastern end of the advanced argillic alteration, locally developed, deformed quartz veins contain anomalous Mo (294 ppm) and Se (9.3 ppm) in association with muscovite alteration (GS-12-159A; Table 2). This zone of anomalous alteration may represent a continuation of the Rattle Brook alteration zone.

### WHITE MOUNTAIN POND

The White Mountain Pond occurrence is a zone of white mica alteration, consisting of muscovite and paragonite, associated with anomalous Au, As, Mo and Se. The zone is exposed along an ATV trail and consists of a 4- to 5-m-wide zone of bleached, white mica ± pyrite alteration, hosted within variably deformed felsic volcanic rocks of the Marystown Group, close to the intrusive margin of the Burin Knee granite. The zone has a northeast trend and can be traced intermittently along strike for 800 m before it becomes obscured by glacial cover. At the southwestern end of the exposed alteration, metre-scale rusty-weathering, vuggy-textured white crystalline quartz veins are exposed (Plate 9). Sampling failed to identify any significant gold values, but to the immediate southwest and upstream of the alteration, a regional lake-sediment sample is anomalous with respect to gold (5 ppb). Near the northeastern end of the defined alteration zone, weakly anomalous Au, As, Mo and Se values are associated with muscovite–pyrite alter-

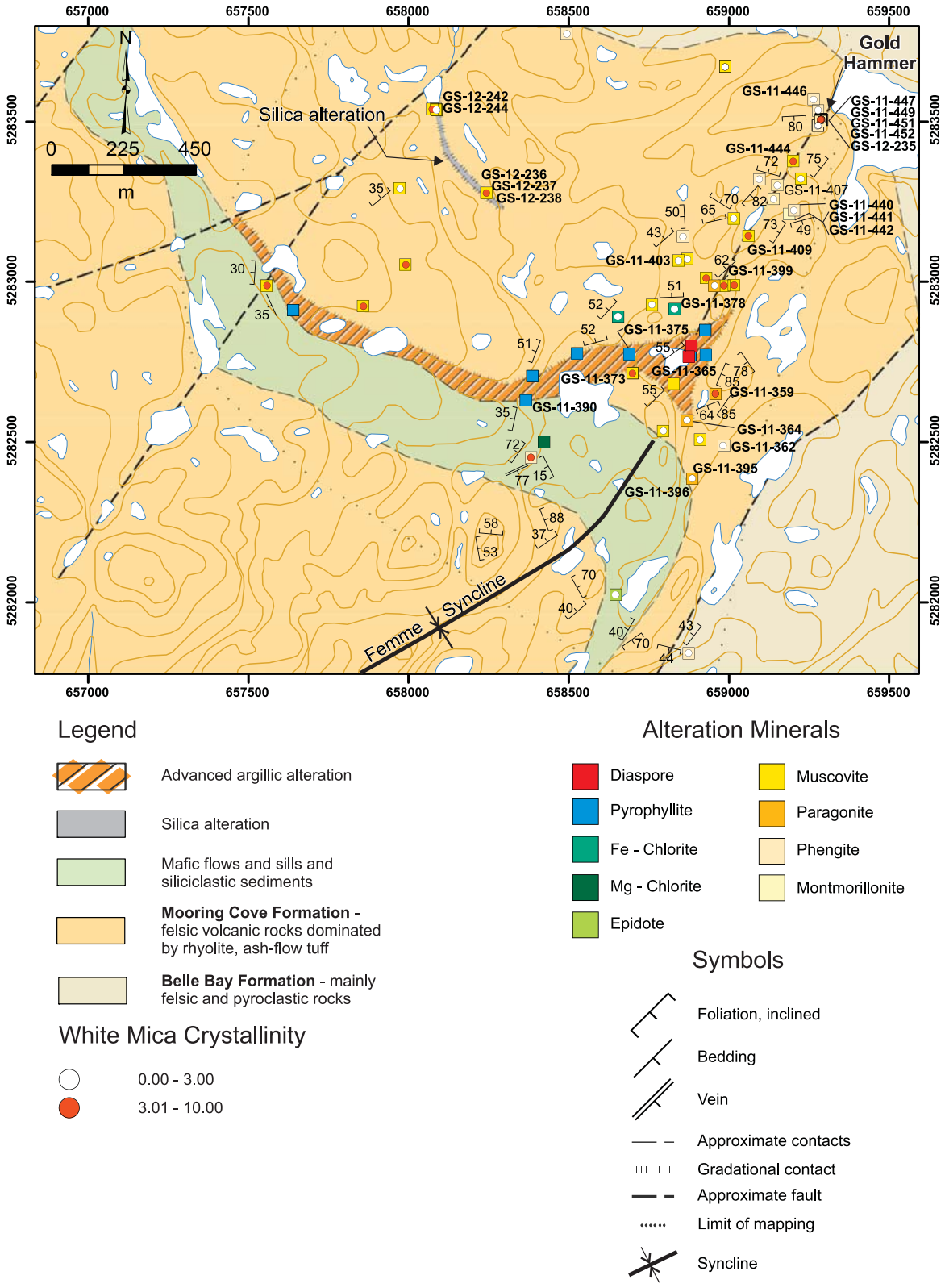


**Figure 6.** *Regional geology map outlining the distribution of the advanced argillic alteration at the Gold Hammer prospect (base-map geology modified from O'Brien* et al.*, 1984). Also shown are the sample locations with their corresponding dominant mineral phase as determined by VIRS, along with the white mica crystallinity of the various white mica phases; red dots denote high-temperature phases. Labelled samples correspond to geochemical analyses in Table 1.*

**Plate 7.** *Pyrophyllite–diaspore alteration developed within a volcaniclastic unit at the eastern end of the advanced argillic alteration near the Gold Hammer prospect.*

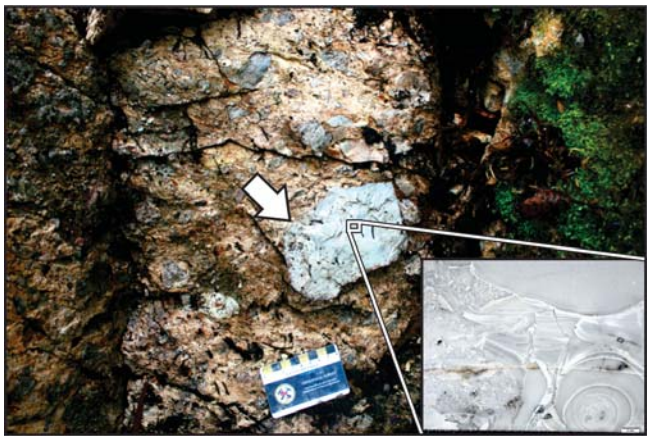

**Plate 8.** *Angular fragment of silica alteration (arrow) of an inferred hydrothermal origin, contained within a volcaniclastic unit overlying the advanced argillic alteration, Gold Hammer prospect. Note the finely laminated nature of the silica alteration shown in the inset.*

ation developed within a fragmental volcanic unit (GS-11-270; Table 2).

## RED HARBOUR

Sampling of exposed alteration zones along the main Burin Highway identified a previously unrecognized zone of pyrophyllite alteration in a roadcut, about 3.2 km north of the Red Harbour exit (Figure 1). The alteration is hosted within a relatively narrow zone that appears to be localized along a north–northeast-trending linear that crosscuts the road at an oblique angle. Within the roadcut, dark purple crystal tuff is bleached to pale beige, representing the loss of primary hematite within the protolith, which is accompanied by the development of pyrophyllite alteration. Follow-up investigations along the Red Harbour River East, north of

**Table 2.** Geochemical samples collected in relation to mapping of select zones of advanced argillic alteration. Note: N/A = not analyzed; - = below detection limit; coordinates are listed in NAD27, Zone 21

| Sample | UTM E | UTM N | Prospect | Description | | Alteration Mineralogy | Au | Ag | As | Ba | Be | Bi | Ca | Cd | Cu | Fe | Hg | K | Mn | Mo | Na | Pb | S | Sb | Se | Te | Ti | Tl | W | Zn |
|---|---|---|---|---|---|---|---|---|---|---|---|---|---|---|---|---|---|---|---|---|---|---|---|---|---|---|---|---|---|---|
| | | | | | | | ppb | ppm | ppm | ppm | ppm | ppm | % | ppm | ppm | % | ppm | % | % | ppm | % | ppm | % | ppm | ppm | ppm | ppm | ppm | ppm | ppm | ppm |
| | | | | | Detection limit | | 5 | 0.2 | 2 | 1 | 0.1 | 0.1 | 0.0 | 0.1 | 1 | 0.01 | 1 | 0.01 | 0.01 | 1 | 0.01 | 1 | 0.01 | 0.1 | 0.1 | 0.1 | 1 | 0.01 | 1 | 1 |
| GS-12-11 | 661624 | 5257261 | Rattle Brook | beige silica alteration | | Muscovite | - | - | - | 25 | - | 0.6 | - | - | - | 0.11 | - | 0.08 | 7 | - | 0.04 | - | 0.00 | 14.5 | 0.1 | 0.2 | 5484 | - | 20 | 2 |
| GS-12-12 | 661641 | 5257284 | Rattle Brook | grey silica alteration | | Muscovite | - | - | 2 | 12 | - | 0.2 | - | - | 9 | 0.06 | - | 0.02 | 9 | - | 0.02 | - | 0.00 | 0.5 | - | 0.2 | 297 | - | - | 1 |
| GS-12-16 | 661480 | 5257332 | Rattle Brook | deformed mafic dyke | | FeChlorite | - | - | 11 | 51 | 0.9 | 0.1 | 0.1 | - | 50 | 13.10 | - | 0.05 | 865 | 9 | 0.08 | 29 | 0.73 | - | 0.5 | - | 6796 | - | - | 92 |
| GS-12-19 | 660724 | 5257628 | Rattle Brook | quartz-alunite alteration | | K Alunite | - | - | 4 | 13 | - | 0.5 | - | - | 4 | - | - | 0.42 | 4 | - | 0.89 | 3 | 1.03 | - | 0.3 | 0.7 | 186 | - | - | 2 |
| GS-12-20 | 660696 | 5257646 | Rattle Brook | grey silica alteration | | Muscovite,Na Alunite | - | - | - | 10 | - | 0.1 | - | - | 2 | 0.10 | - | - | 21 | - | 0.02 | - | 0.02 | 3.4 | - | 0.1 | 895 | - | - | 2 |
| GS-12-85 | 660379 | 5257405 | Rattle Brook | grey silica alteration | | | - | - | - | 139 | - | - | - | - | 11 | 0.08 | - | - | 6 | - | 0.01 | - | 0.00 | 1.9 | - | 0.2 | 2845 | - | - | 2 |
| GS-12-147 | 662121 | 5256711 | Rattle Brook | silica-pyrite alteration | | Muscovite,Epidote | - | - | 4 | 19 | 1.2 | 0.7 | 1.1 | 0.7 | 7 | 6.00 | - | 0.21 | 752 | - | 2.53 | 8 | 4.13 | - | 0.9 | 0.5 | 5806 | 0.30 | - | 66 |
| GS-12-150 | 662192 | 5256747 | Rattle Brook | silica-pyrite alteration with up to 20-30% pyrite | | Muscovite,Pyrophyllite | 27 | 0.8 | - | 33 | - | - | N/A | N/A | 11 | 11.00 | N/A | N/A | 101 | 11 | - | 50 | N/A | 1.1 | - | N/A | 1770 | - | 2 | 15 |
| GS-12-155 | 662192 | 5256747 | Rattle Brook | white mica alteration | | Muscovite | - | - | - | 48 | 0.7 | - | 0.9 | - | 21 | 0.69 | - | 0.31 | 95 | - | 0.44 | - | 0.01 | - | - | 0.2 | 3214 | 0.20 | - | 9 |
| GS-12-159A | 662965 | 5256886 | Rattle Brook | deformed quartz vein with trace molybdenum | | Muscovite,FeMgChlorite | 11 | 0.2 | 8 | 41 | 0.9 | 1.0 | 0.0 | - | 9 | 1.56 | - | 0.16 | 105 | 294 | 0.17 | 160 | 1.42 | 1.4 | 9.3 | 1.8 | 1445 | 0.20 | - | 53 |
| GS-11-236 | 645541 | 5256863 | White Mountain Pond | white mica alteration | | Phengite | - | N/A | 16 | 927 | 1.6 | - | N/A | - | 5 | 1.14 | N/A | N/A | 400 | 5 | 1.60 | 12 | N/A | 0.6 | - | N/A | 2356 | - | 1 | 14 |
| GS-11-237 | 646088 | 5256685 | White Mountain Pond | white mica alteration | | Paragonite,Montmorillonite | - | - | 3 | 530 | 0.8 | - | - | - | - | 0.38 | - | 0.24 | 3 | - | 0.59 | 2 | 0.00 | 0.5 | 0.4 | - | 949 | - | - | 2 |
| GS-11-238 | 646352 | 5256802 | White Mountain Pond | silica-pyrite alteration | | Muscovite | - | - | 5 | 1076 | 1.5 | 0.2 | 0.7 | 0.2 | 2 | 0.66 | - | 2.15 | 171 | 2 | 2.04 | 15.5 | 0.61 | 1.1 | - | 0.2 | 1097 | 0.40 | 2 | 50 |
| GS-11-261 | 645827 | 5256454 | White Mountain Pond | vuggy white quartz-chlorite veining with minor rusting | | | - | - | 5 | 25 | - | - | 0.4 | - | 7 | 0.36 | - | 0.03 | 425 | - | - | 4 | 0.01 | 0.3 | 0.2 | - | 164 | 0.86 | 3 | 23 |
| GS-11-262 | 645867 | 5256454 | White Mountain Pond | chlorite-pyrite alteration; wall rock to quartz vein in sample GS-11-261 | | Muscovite,FeMgChlorite | - | - | 7 | 1268 | 1.9 | 0.3 | 0.3 | - | 5 | 3.33 | - | 0.27 | 516 | 7 | 0.93 | 11 | 0.04 | 2.0 | 0.7 | - | 5652 | 0.18 | 2 | 83 |
| GS-11-263 | 645867 | 5256454 | White Mountain Pond | white quartz-chlorite veining with minor rusting | | | - | - | 5 | 168 | 0.3 | - | 0.2 | - | 7 | 1.05 | - | 0.10 | 77 | 1 | 0.13 | 3 | 0.13 | 0.6 | 0.2 | - | 2092 | 0.42 | 3 | 12 |
| GS-11-264 | 645856 | 5256440 | White Mountain Pond | white mica-pyrite alteration | | Paragonite | - | - | 25 | 1104 | 1.8 | 0.2 | - | - | 5 | 2.13 | - | 0.31 | 20 | - | 0.55 | 6 | 0.04 | 1.3 | 0.5 | - | 1987 | - | - | 11 |
| GS-11-265 | 646206 | 5256086 | White Mountain Pond | silica-pyrite alteration | | Phengite | - | N/A | 9 | 837 | 1.4 | - | N/A | - | 3 | 1.08 | N/A | N/A | 356 | - | 1.50 | 10 | N/A | 0.4 | - | N/A | 1440 | - | - | 23 |
| GS-11-268 | 646530 | 5256876 | White Mountain Pond | chlorite-pyrite alteration | | Muscovite | - | N/A | - | 858 | 2.0 | - | N/A | - | 7 | 3.06 | N/A | N/A | 527 | - | 1.00 | 6 | N/A | 0.6 | - | N/A | 4484 | - | 1 | 73 |
| GS-11-269 | 646511 | 5256875 | White Mountain Pond | white mica-pyrite alteration | | Paragonite | 7 | N/A | 5 | 597 | 1.8 | - | N/A | - | 15 | 4.88 | N/A | N/A | 163 | 1 | 0.71 | 16 | N/A | 0.9 | - | N/A | 4209 | 0.66 | 2 | 39 |
| GS-11-270 | 646511 | 5256864 | White Mountain Pond | white mica-pyrite alteration | | Muscovite | 58 | 0.3 | 85 | 362 | 1.2 | 0.2 | 0.2 | - | 14 | 2.17 | - | 2.25 | 216 | 38 | 0.41 | 19.6 | 1.31 | 3.5 | 16.0 | 0.9 | 2793 | 0.39 | 6 | 66 |
| GS-11-272 | 647957 | 5256477 | White Mountain Pond | chlorite-white mica alteration | | Phengite,FeChlorite | - | N/A | 9 | 924 | 1.5 | - | N/A | - | 2 | 1.78 | N/A | N/A | 499 | - | 1.10 | 5 | N/A | 0.8 | - | N/A | 1512 | 0.36 | 2 | 40 |
| GS-11-302 | 652186 | 5243073 | Red Harbour River East | white mica-pyrite alteration | | Muscovite,Pyrophyllite | - | N/A | - | 110 | 0.2 | - | N/A | - | 9 | 3.63 | N/A | N/A | 54 | 7 | 0.15 | 4 | N/A | 0.3 | - | N/A | 1352 | - | 3 | 11 |
| GS-12-57 | 652632 | 5243778 | Red Harbour River East | silica-pyrite alteration | | Kaolinite,Muscovite | - | 0.2 | 16 | 37 | 1.4 | - | 2.4 | - | 7 | 4.38 | - | 0.12 | 1020 | - | 2.06 | 27 | 2.02 | - | 1.5 | 0.5 | 4745 | - | - | 151 |
| GS-12-58 | 652632 | 5243778 | Red Harbour River East | beige clay alteration | | Kaolinite | - | - | 26 | 110 | 1.2 | N/A | N/A | N/A | 24 | 3.10 | N/A | N/A | 958 | - | 2.30 | 11 | N/A | 0.6 | - | N/A | 4356 | N/A | - | 46 |
| GS-12-206 | 620730 | 5220027 | Beacon Hill | silica-pyrite alteration | | | - | - | 35 | 411 | - | 1.7 | - | - | 14 | 0.19 | - | - | 4 | - | - | - | 0.01 | 0.9 | 0.2 | 1.9 | 2559 | - | - | 2 |
| GS-12-207 | 620735 | 5220024 | Beacon Hill | silica-pyrite alteration | | K Alunite | - | - | 12 | 90 | 0.1 | 1.9 | - | - | 7 | 0.48 | - | 0.20 | 9 | 3 | 0.50 | 4 | 0.57 | 0.6 | 3.9 | 25.5 | 2171 | - | - | 2 |
| GS-12-210 | 620710 | 5220143 | Beacon Hill | vuggy silica alteration | | Kaolinite, K Alunite | - | - | 9 | 72 | 0.1 | 12.9 | - | - | 4 | 0.24 | - | 0.10 | - | 9 | 0.34 | 5 | 0.27 | 1.9 | 3.3 | 16.4 | 1950 | - | - | 4 |
| GS-12-211 | 620743 | 5220006 | Beacon Hill | silica-pyrite alteration | | Pyrophyllite,Muscovite | - | - | 13 | 11 | 0.3 | 2.7 | - | - | 3 | 1.76 | - | - | 2 | 7 | 0.04 | 3 | 1.55 | 0.9 | 1.8 | 5.2 | 3919 | 0.20 | - | 2 |
| GS-12-214 | 619812 | 5220198 | Beacon Hill | chlorite-pyrite alteration | | FeMgChlorite,Muscovite | - | 0.4 | 20 | 29 | 1.4 | 1.0 | 0.2 | - | 26 | 7.09 | - | 0.30 | 549 | - | 0.16 | 19 | 3.13 | 0.8 | 3.2 | 2.8 | 3306 | 0.20 | - | 47 |

**Plate 9.** *Locally developed rusty-weathering, vuggy, white crystalline quartz veins located at the southwestern end of the White Mountain Pond alteration zone.*

the Burin highway, identified minor kaolinite alteration along strike approximately 800 m to the northeast, but no significant precious metal values were identified in association with the alteration (Table 2).

### BEACON HILL

This area represents another previously known zone of alteration for which little information is available, aside from a brief mention by Marsden and Bradford (2005). The alteration is exposed at the top of a prominent hill with little outcrop exposure where the zone is defined over a maximum width of approximately 200 m. The advanced argillic alteration includes variably developed pyrophyllite, dickite, potassic alunite and kaolinite assemblages, in addition to pervasive silicification. The host rocks are inferred to be felsic volcanic rocks of the Marystown Group. Locally, vuggy-textured silica is developed in association with alunite (Plate 10); but no visible sulphide minerals are developed within the vugs. Limited sampling of the alteration failed to identify any significant precious-metal values, but the alteration is locally anomalous in Te, relative to other prospects in the region (GS-12-210; Table 2). Prospecting in the area has reported anomalous Mo and Zn values of up to 109 and 278 ppm, respectively (Marsden and Bradford, 2005); however evidence of the reported stockwork-style mineralization occurring marginal to the advanced argillic alteration was not observed.

## GEOCHRONOLOGICAL SAMPLING AND RESULTS

Samples were collected in 2011 and 2012 to determine the ages of key units to constrain the formation of epithermal systems. In part, the sampling targeted plutonic rocks that might represent potential heat sources for the hydrothermal systems. The locations and final U/Pb ages are summarized in Figure 7, and UTM's are provided in Table 3. In total, six samples were investigated, all of which yielded small prismatic zircons that, in each case, appear to represent a single-age igneous population displaying fine-scale growth zoning (Plate 11). This interpretation is confirmed by the isotopic data that are concordant and overlapping. New analyses of archived zircon (Sample TK77-23), previously reported by Krogh *et al*. (1988) to have an age of 608 +20/-7 Ma, were carried out to test this older age limit for rocks of the Marystown Group. A new sample was also collected from the reported sample site for TK77-23 (Krogh *et al*., 1988) as the original location for this sample was thought to have been erroneously reported (S.J. O'Brien, personal communication, 2013).

**Plate 10.** *Photograph of the typical vuggy-textured silica in association with alunite–kaolinite alteration from the Beacon Hill prospect.*

### U/Pb ZIRCON CA-TIMS ANALYTICAL PROCEDURE

The zircon grains analyzed were selected from mineral concentrates, using tweezers, under the microscope according to criteria of clarity, euhedral crystal form and lack of inclusions. All grains were chemically abraded using the Mattinson (2005) chemical abrasion thermal ionization mass spectrometry (CA-TIMS) technique. The selected zircon crystals were annealed at 900°C for 36 hours prior to etching in concentrated hydrofluoric acid in a pressure bomb at 200°C for a few hours. This procedure is designed to remove any altered domains throughout the crystal that may have undergone Pb loss. This effective and simple procedure has now largely replaced physical abrasion (Krogh, 1982) for zircon analysis.

For each sample, a small number of zircon grains were grouped into fractions of like morphology, and analyzed by

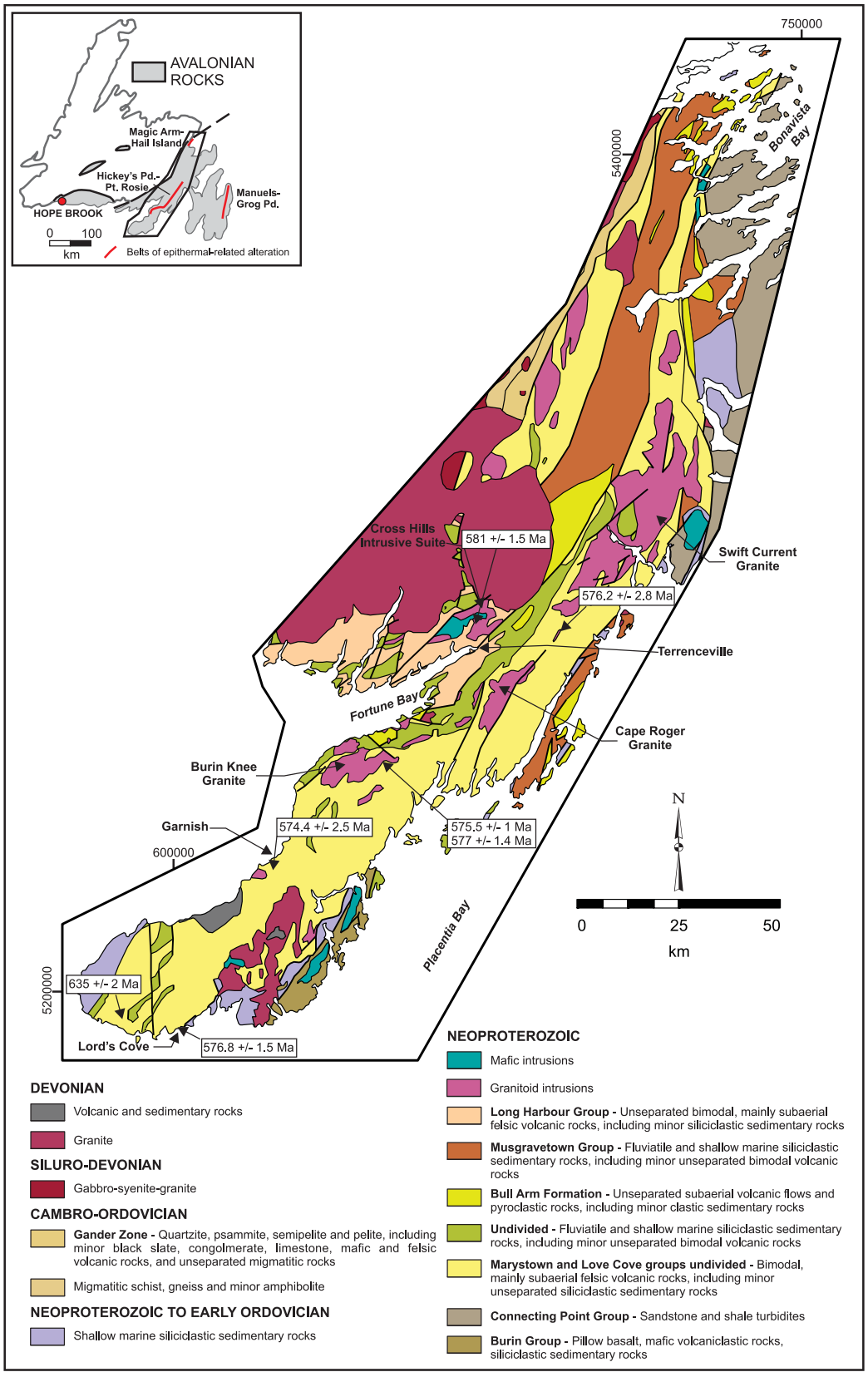


**Figure 7.** *Regional geology map of the western Avalon Zone showing geochronological sample locations collected as part of this study and their corresponding ages (*modified from *O'Brien* et al.*, 1998; coordinates are listed in NAD 27, Zone 21).*

**Table 3.** U/Pb data from rocks from the Burin Peninsula. UTM's listed for each sample location are provided in NAD 27, Zone 21 coordinates

| | | Concentration | | Measured | | Corrected Atomic Ratios (c) | | | | | | Age [Ma] | | |
|---|---|---|---|---|---|---|---|---|---|---|---|---|---|---|
| Fraction | Weight [mg] (a) | U [ppm] | Pb rad (b) | total common Pb [pg] | $^{206}Pb/^{204}Pb$ | $^{208}Pb/^{206}Pb$ | $^{206}Pb/^{238}U$ | | $^{207}Pb/^{235}U$ | | $^{207}Pb/^{206}Pb$ | | $^{206}Pb/^{238}U$ | $^{207}Pb/^{235}U$ | $^{207}Pb/^{206}Pb$ |
| **GS12-63: Medium-grained granite – Peter Brook Granite (587709E, 5193944N)** | | | | | | | | | | | | | | | |
| Z1 10 clr euh prm | 0.015 | 280 | 32.2 | 47 | 619 | 0.1934 | 0.10644 | 76 | 0.9141 | 72 | 0.06229 | 24 | 652 | 659 | 684 |
| Z2 2 clr euh prm | 0.003 | 404 | 46.7 | 5.0 | 1579 | 0.2369 | 0.10360 | 56 | 0.8653 | 58 | 0.06058 | 26 | 635 | 633 | 624 |
| Z3 4 clr euh prm | 0.006 | 316 | 35.8 | 26 | 498 | 0.2074 | 0.10372 | 62 | 0.8704 | 76 | 0.06087 | 38 | 636 | 636 | 635 |
| Z4 5 clr euh prm | 0.007 | 217 | 24.6 | 11 | 1002 | 0.2140 | 0.10330 | 62 | 0.8668 | 62 | 0.06085 | 36 | 634 | 634 | 634 |
| **GS12-384: Medium-grained granodiorite (671813E, 5287658N)** | | | | | | | | | | | | | | | |
| Z1 2 clr euh prm | 0.003 | 89 | 9.1 | 8.8 | 196 | 0.1992 | 0.09424 | 62 | 0.7781 | 136 | 0.05988 | 94 | 581 | 584 | 599 |
| Z2 5 clr euh prm | 0.007 | 384 | 39.8 | 4.7 | 3619 | 0.2205 | 0.09423 | 54 | 0.7728 | 42 | 0.05948 | 20 | 581 | 581 | 585 |
| Z3 4 clr euh prm | 0.006 | 393 | 40.5 | 3.9 | 3566 | 0.2127 | 0.09419 | 68 | 0.7656 | 60 | 0.05895 | 26 | 580 | 577 | 565 |
| Z4 2 clr euh prm | 0.003 | 180 | 18.4 | 4.8 | 680 | 0.1950 | 0.09452 | 72 | 0.7721 | 88 | 0.05925 | 58 | 582 | 581 | 576 |
| Z5 6 sml prm | 0.009 | 370 | 38.1 | 65 | 323 | 0.2085 | 0.09434 | 50 | 0.7738 | 54 | 0.05949 | 36 | 581 | 582 | 585 |
| **GS11-169: Quartz diorite (650132E, 5253625N)** | | | | | | | | | | | | | | | |
| Z1 4 clr euh prm | 0.006 | 252 | 27.4 | 3.0 | 2918 | 0.2980 | 0.09313 | 64 | 0.7597 | 58 | 0.05916 | 46 | 574 | 574 | 573 |
| Z2 2 clr euh prm | 0.003 | 328 | 36.0 | 2.7 | 2152 | 0.3044 | 0.09355 | 48 | 0.7647 | 42 | 0.05929 | 24 | 576 | 577 | 578 |
| Z3 5 prm + frags | 0.007 | 111 | 11.9 | 5.1 | 986 | 0.2665 | 0.09363 | 42 | 0.7670 | 40 | 0.05942 | 28 | 577 | 578 | 582 |
| Z4 2 prm frags | 0.003 | 95 | 10.3 | 3.3 | 523 | 0.2816 | 0.09384 | 58 | 0.7674 | 68 | 0.05931 | 46 | 578 | 578 | 578 |
| Z5 5 prm frags | 0.007 | 58 | 6.4 | 3.1 | 839 | 0.3072 | 0.09364 | 50 | 0.7658 | 64 | 0.05932 | 42 | 577 | 577 | 579 |
| **GS-11-168: Fine-grained granodiorite (649633E, 5254018N)** | | | | | | | | | | | | | | | |
| Z1 5 clr euh prm | 0.007 | 74 | 8.1 | 2.4 | 1382 | 0.3028 | 0.09343 | 38 | 0.7589 | 50 | 0.05891 | 34 | 576 | 573 | 564 |
| Z2 2 clr euh prm | 0.003 | 115 | 12.6 | 1.3 | 1542 | 0.3091 | 0.09336 | 40 | 0.7578 | 44 | 0.05887 | 28 | 575 | 573 | 562 |
| Z3 2 clr euh prm | 0.003 | 278 | 30.9 | 1.7 | 2847 | 0.3192 | 0.09349 | 48 | 0.7646 | 42 | 0.05931 | 28 | 576 | 577 | 579 |
| **GS12-335: Felsic lapilli tuff (Marystown Group) (600924E, 5192607N)** | | | | | | | | | | | | | | | |
| Z1 3 euh prm | 0.004 | 137 | 17.0 | 2.6 | 1392 | 0.4840 | 0.09374 | 58 | 0.7654 | 68 | 0.05922 | 44 | 578 | 577 | 575 |
| Z2 4 euh prm | 0.006 | 144 | 16.0 | 1.9 | 2641 | 0.3251 | 0.09337 | 74 | 0.7645 | 98 | 0.05939 | 64 | 575 | 577 | 581 |
| **GS11-428: Felsic tuff (Marystown Group) (691820E, 5285155N)** | | | | | | | | | | | | | | | |
| Z1 1 long prm + frag | 0.003 | 647 | 85.8 | 41 | 277 | 0.6976 | 0.08750 | 82 | 0.7114 | 84 | 0.05897 | 52 | 541 | 546 | 566 |
| Z2 5 sml prm frags | 0.005 | 764 | 84.1 | 7.1 | 2856 | 0.4649 | 0.08386 | 68 | 0.6844 | 42 | 0.05919 | 32 | 519 | 529 | 574 |
| Z3 2 clr sml equ | 0.002 | 48 | 5.4 | 9.0 | 81 | 0.3397 | 0.09380 | 116 | 0.7888 | 826 | 0.06099 | 590 | 578 | 590 | 639 |
| Z4 5 clr sml equ | 0.005 | 82 | 10.1 | 26 | 113 | 0.4466 | 0.09403 | 54 | 0.7736 | 340 | 0.05967 | 244 | 579 | 582 | 592 |

| | | | | | | | | | | | | | | | |
|---|---|---|---|---|---|---|---|---|---|---|---|---|---|---|---|
| Z5 4 clr sml equ | 0.004 | 126 | 14.8 | 8.3 | 373 | 0.4041 | 0.09330 | 54 | 0.7629 | 68 | 0.05930 | 46 | 575 | 576 | 578 |
| Z6 3 clr sml prm | 0.003 | 32 | 3.7 | 8.2 | 86 | 0.3651 | 0.09361 | 108 | 0.7817 | 532 | 0.06057 | 382 | 577 | 586 | 624 |
| Z7 4 clr sml equ | 0.004 | 56 | 6.2 | 22 | 77 | 0.3368 | 0.09332 | 96 | 0.7451 | 880 | 0.05791 | 634 | 575 | 565 | 526 |
| Z8 6 clr sml equ | 0.006 | 41 | 5.1 | 3.2 | 465 | 0.4770 | 0.09286 | 70 | 0.7625 | 228 | 0.05955 | 170 | 572 | 575 | 587 |
| | | | | | | | | | | | | | | | |
| **TK77-23: Ash-flow tuff (623504E, 5228215N)*** | | | | | | | | | | | | | | | |
| Z1 3 sml euh prm | 0.004 | 174 | 20.2 | 8.0 | 589 | 0.3810 | 0.09318 | 62 | 0.7609 | 62 | 0.05922 | 36 | 574 | 575 | 575 |
| Z2 2 sml euh prm | 0.003 | 38 | 4.5 | 4.0 | 187 | 0.4185 | 0.09308 | 106 | 0.7599 | 202 | 0.05921 | 144 | 574 | 574 | 575 |
| Z3 5 sml euh prm | 0.007 | 63 | 7.5 | 1.8 | 1620 | 0.3701 | 0.09575 | 52 | 0.7872 | 44 | 0.05963 | 26 | 589 | 590 | 590 |
| Z4 2 sml best prm | 0.003 | 86 | 10.0 | 14 | 124 | 0.3933 | 0.09323 | 68 | 0.7608 | 226 | 0.05919 | 160 | 575 | 574 | 574 |

Notes: All zircon was chemically abraded (Mattinson, 2005) prior to dissolution. Z–zircon; 2,4 number of grains in analysis; prm, prism; sml, small; euh, euhedral; frag, fragments; clr, clear; equ, equant.

a. Weights of grains were estimated, with potential uncertainties of 25–50% for these small samples.

b. Radiogenic lead

c. Atomic ratios corrected for fractionation, spike, laboratory blank of 0.6-2 picograms (pg) common lead, and initial common lead at the age of the sample calculated from the model of Stacey and Kramers (1975), and 0.3 pg U blank. Two sigma uncertainties are reported after the ratios and refer to the final digits.

* : UTM's determined from description of original sample location of TK77-23, 4.8 km east of western exit to Garnish on the Burin highway.




**Plate 11.** *Cathodoluminescence images of zircon crystals with igneous growth-zoning and representative of the type analyzed from each sample. A. GS12-63, B. GS12-384, C. GS11-169, D. GS11-168, E. GS12-335, F. GS11-428, G. TK77-23. Scale bar applies to all samples.*

TIMS. At an age of *ca.* 570 Ma, for clear, high-quality zircon, this amounts to 2 to 5 grains of zircon per fraction. These etched zircon fractions were washed in distilled nitric acid, then double-distilled water, prior to loading in Krogh-type TEFLON dissolution bombs. A mixed $^{205}Pb/^{235}U$ tracer was added in proportion to the sample weight, along with *ca.* 15 drops of distilled hydrofluoric acid, then the bomb was sealed and placed in an oven at 210°C for 5 days. Ion exchange was carried out according to the procedure of Krogh (1973), with modified columns and reagent volumes scaled down to one tenth of those reported in 1973. The purified Pb and U were collected in a clean beaker in a single drop of ultrapure phosphoric acid.

Lead and uranium are loaded together on outgassed single Re filaments with silica gel and dilute phosphoric acid. Mass spectrometry is carried out using a multi-collector MAT 262. The faraday cups are calibrated with NBS 981 lead standard and the ion-counting secondary electron multiplier (SEM) detector is calibrated against the faraday cups by measurement of known Pb isotopic ratios. The small

amounts of Pb were measured by peak jumping on the SEM, with measurement times weighted according to the amounts of each mass present. The U was measured by peak jumping on the SEM. A series of sets of data are measured in the temperature range 1400 to 1550°C for Pb and 1550 to 1640°C for U, and the best sets are combined to produce a mean value for each ratio. The measured ratios are corrected for Pb and U fractionation of 0.1%/ amu and 0.03%/ amu, respectively, as determined from repeat measurements of NBS standards. The ratios are also corrected for laboratory procedure blanks (1 to 2 picograms - Pb, 0.3 picogram - U) and for common Pb above the laboratory blank with Pb of the composition predicted by the two- stage model of Stacey and Kramers (1975) for the age of the sample. Ages are calculated using the decay constants recommended by Jaffey *et al.* (1971). The uncertainties on the isotopic ratios are calculated and are reported as two sigma (Table 3). The age of each rock is reported as the weighted average of the $^{206}Pb/^{238}U$ ages calculated using ISOPLOT, with the uncertainty reported at the 95% confidence interval.

As a check on the accuracy of the entire laboratory procedure, results of nine U/Pb analyses of the TEMORA zircon standard (Black *et al.,* 2003), carried out during the time of measurement of these samples using the same detector and measurement conditions, are shown in Figure 8. Eight of nine analyses overlap and yield a weighted average $^{206}Pb/^{238}U$ age of 416.84 Ma (MSWD=0.18), which is in close agreement with the published value of 416.75 Ma (Black *et al.,* 2003). The one lower analysis is interpreted to display minor Pb-loss.

## NEOPROTEROZOIC INTRUSIVE ROCKS

### Host Rock to the Peter Brook Prospect

The Peter Brook prospect is one of the first reported occurrences of low-sulphidation-style epithermal veining on the Burin Peninsula (Evans and Vatcher, 2010). Well-developed colloform–crustiform chalcedonic silica veins and related breccias, assaying up to 1.2 g/t Au and 130.4 g/t Ag (Evans and Vatcher, 2010), are hosted within a medium-grained granite that is grouped with late Proterozoic intrusions on regional geological maps of the area (O'Brien *et al*., 1977). The low-sulphidation epithermal veining at the prospect is developed as a northeast–southwest-trending 10- to 15-m-wide zone exposed within a stream bed and is elsewhere obscured by extensive surficial cover. The medium-grained granite displays localized zones of brecciation and has muscovite–illite alteration in wall rock immediately adjacent to the veins (Plate 12). The granite intrusion is flanked to the southwest by thinly bedded, red and green, fine-grained sandstone, but the nature of this contact remains undefined.

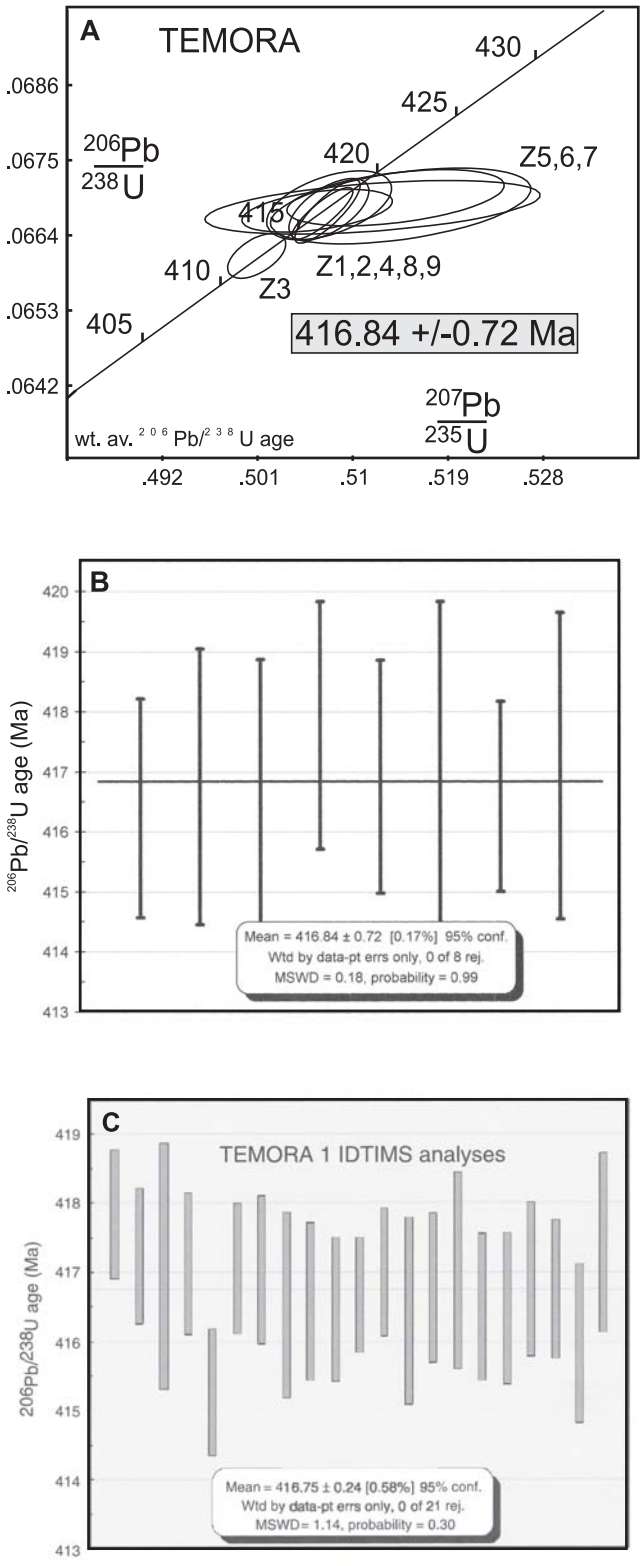


**Figure 8.** *A) Concordia diagram illustrating nine zircon analyses of the TEMORA international standard; B) Diagram showing the $^{206}Pb/^{238}U$ ages of the eight analyses; C) Diagram showing the $^{206}Pb/^{238}U$ ages obtained by Black* et al. *(2003).*

**Plate 12.** *A representative sample of the altered granite hosting well-developed colloform–crustiform-banded chalcedonic silica veins associated with the low-sulphidation related mineralization at the Peter Brook prospect.*

Sample GS12-63 was collected from the medium-grained host granite. Three fractions of 2 to 5 grains are concordant, overlapping and they yield a weighted average $^{206}Pb/^{238}U$ age of 635 ± 2 Ma (MSWD = 0.49; Figure 9A). One fraction (of 10 grains) is discordant and displaced to an older age. It either contains an older grain, or an older core in one or more grains.

### Granite North of Fortune Bay (Previously grouped with the Cross Hills Intrusive Suite)

This sample was collected to provide a better age constraint on the Cross Hills Intrusive Suite, which is close to the advanced argillic alteration at the Gold Hammer prospect (*see* above), and is a possible heat source for the formation of the alteration. Previous attempts to date the Cross Hills Intrusive Suite produced a preliminary U/Pb age of 547 +3/-6 Ma (Tuach, 1991), however, were hampered by the high uranium content and poor quality of the zircon crystals. Sample GS12-384 was collected along the road between Terrenceville and Grand le Pierre and was chosen on the basis of its low radioactivity as determined using a handheld scintillometer. The sample was a medium-grained granodiorite from which five analyses consisting of fractions containing 2 to 6 prisms were carried out; all are concordant and overlap. These yield a weighted average $^{206}Pb/^{238}U$ age of 581 ± 1.5 Ma (MSWD = 0.15; Figure 9B). This age is demonstrably older than previous results from granites of the Cross Hills Intrusive Suite, indicating that revision of map units in the area is needed.

### Stewart Prospect

Previous mapping in the area of the Stewart prospect (*cf.* Sparkes, 2012 and references therein) defined an altered quartz diorite unit that has a close spatial relationship with the development of advanced argillic alteration and related mineralization. Sample GS11-169 was collected from an outcrop of the altered quartz diorite exposed within an exploration trench at the Stewart prospect. This sample was collected to test the age of this intensely altered intrusion relative to the generally unaltered intrusions of the Burin Knee granite (GS11-168; *see* below). Five analyses, each using between 2 to 5 zircon prisms are concordant and overlap, however, analysis Z1 is noticeably younger than the others with an age of 574 Ma. The age determined from analyses Z2 to Z5 is 577 ± 1.4 Ma (MSWD=0.2; Figure 9C).

A sample from a fine-grained granodiorite phase of the Burin Knee granite (Figure 2) was collected from the western end of the same exploration trench as the sample of the altered quartz diorite. This sample was collected to test its age relative to the altered quartz diorite, and to test the idea that these intrusions correlate with the Swift Current Granite. Sample GS11-168 produced three concordant overlapping analyses that provide a weighted average $^{206}Pb/^{238}U$ age of 575.5 ± 1 Ma (MSWD=0.15; Figure 9D). The ages from the two samples at the Stewart prospect are indistinguishable within analytical error.

## NEOPROTEROZOIC VOLCANIC ROCKS

### Marystown Group (Southwestern Burin Peninsula)

The volcanic sequence at the Lord's Cove area was sampled to test the previously reported age of 608 +20/-7 Ma (Krogh *et al*., 1988; Figure 7). However, unpublished field information (S.J. O'Brien, personal communication, 2013) suggests that this sample (TK77-23) actually came from a different location than that reported; some 40 km to the northeast in the area of Garnish. Sample GS12-335 was collected along the road in Lord's Cove, and is a fine-grained felsic lapilli tuff from which two analyses consisting of 3 to 4 zircon prisms are concordant and overlap and produce a weighted average $^{206}Pb/^{238}U$ age of 576.8 ± 2.6 Ma (MSWD=0.62; Figure 9E).

### Marystown Group (Monkstown Road)

Sample GS11-428 was collected from a quarry on Monkstown Road, approximately 1 km southwest of the Tower prospect (Figure 5). The sample, which consists of pale purple fine-grained felsic tuff of the Marystown Group, was collected to compare its age with the *ca.* 572 Ma age obtained from the host rock of the Hickey's Pond prospect farther to the north (O'Brien *et al*., 1999). Of the eight analyses carried out, two are discordant whereas the other six are concordant and overlap. Several analyses have large uncertainties on the $^{207}Pb/^{235}U$ ratio (and age), due to the very

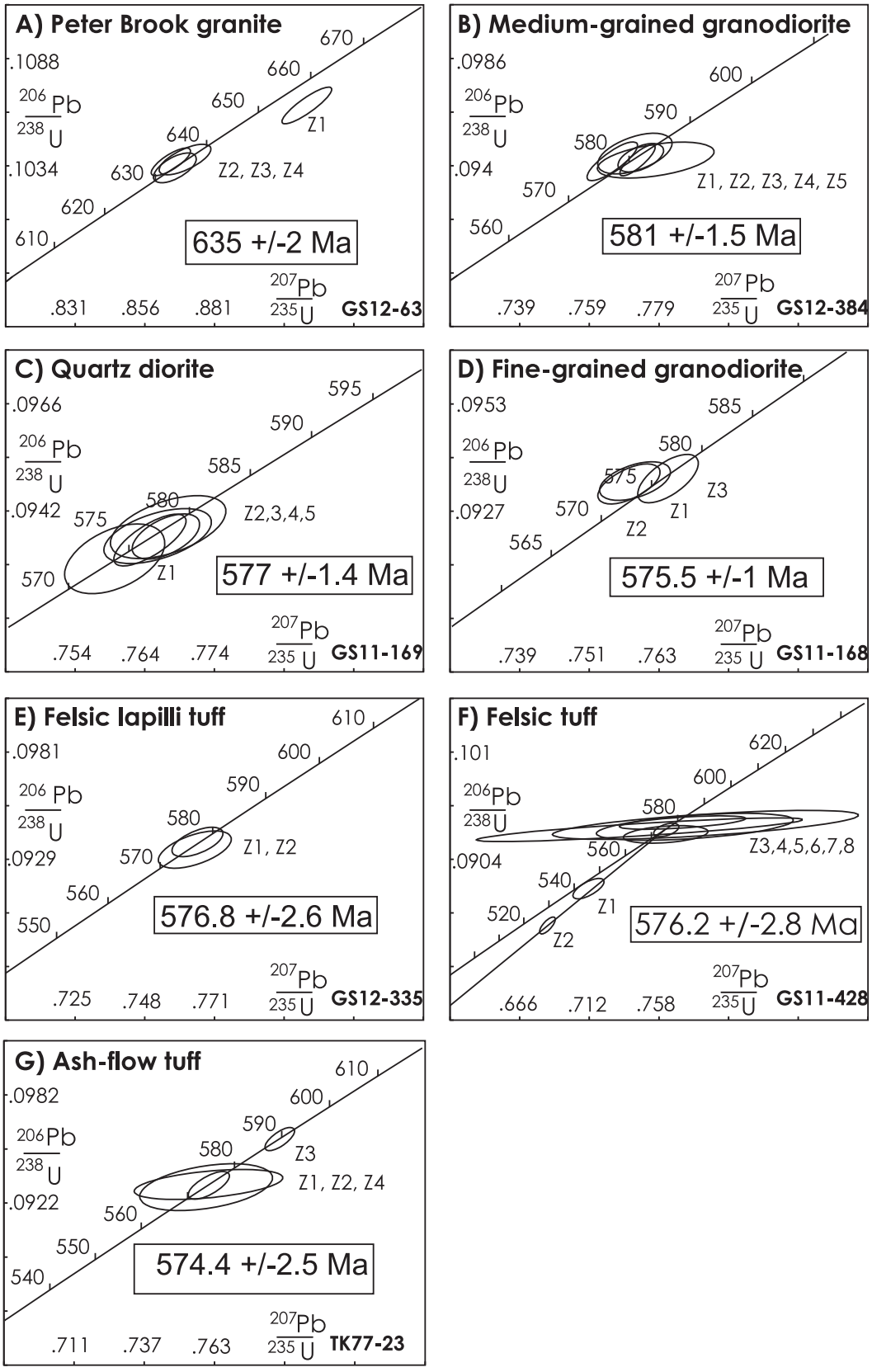


**Figure 9.** *Concordia diagrams of U/Pb results of zircon analyses from samples from the Burin Peninsula. Error ellipses are at the 2σ level. Refer to Table 3 for sample locations and descriptions.*

small amounts of $^{207}Pb$ in the crystals, which is less than one picogram in some analyses. Analyses Z3 to Z8 yield a weighted average $^{206}Pb/^{238}U$ age of 576.2 ± 2.8 Ma (MSWD=1.6; Figure 9F).

**Marystown Group (Archived Sample TK77-23 from Krogh *et al.*, 1988)**

As discussed above, the Krogh *et al.* (1988) sample, TK77-23, is located some 40 km northeast of its originally reported location, and comes from a roadcut approximately 4.8 km east of the western Garnish exit (Figure 7). To resolve questions about this older age, four new analyses from the archived sample were completed. These analyses demonstrate the presence of older crystals in this rock, and this is the likely explanation for the previously published age of 608 Ma. Analysis Z3 likely has an older crystal or an older core in one or more crystals, possibly derived from an older volcanic sequence. Three analyses, of 2 or 3 zircon prisms each, are concordant and overlap and yield an age of 574.4 ± 2.5 Ma (MSWD= 0.03; Figure 9G). This is essentially indistinguishable from the ages determined for other samples from the Marystown Group.

## DISCUSSION

### ALTERATION SIGNATURES

The alunite-dominated alteration of the Monkstown Road Belt is locally accompanied by pyrophyllite and dickite, indicative of high-temperature-formation (200–350° C) acidic conditions at relatively shallow crustal levels (Meyer and Hemley, 1967; Arribas, 1995; Hedenquist and Taran, 2013). The predominance of alunite throughout the belt, with little variation in the mineralogy of the alteration along the exposed strike length of the zone, suggests a similar level of exposure throughout the hydrothermal system, with no evidence of the tilting inferred for some other areas of the Burin Peninsula (*e.g.,* Stewart prospect, Sparkes, 2012). However, preliminary data from samples obtained at lower elevations (present-day) appear to be dominated by more potassic alunite, whereas higher elevations are dominated by more sodic alunite. Data from epithermal systems elsewhere suggest that the higher temperature portion of the epithermal systems are dominated by sodic alunite (*e.g.,* Chang *et al*., 2011), and therefore implies that the higher topographic levels of the Monkstown Road Belt represent areas of higher paleotemperatures. Further work is required to confirm the development of potassic alunite at lower elevations, and evaluate the significance of this pattern.

The Tower prospect has a similar style of alteration to the adjacent Monkstown Road Belt, with sodic alunite dominating in most areas. Limited sampling of the advanced argillic alteration, exposed to the northeast at Chimney Falls and Hickey's Pond prospects (Figure 3), suggests that these areas are also dominated by sodic alunite. The Tower prospect seems to have at least two stages of hydrothermal alteration, and it is the second stage, dominated by alunite–pyrite, that is linked to metal enrichment. There is as yet no obvious explanation for the differences in gold abundance amongst the Monkstown Road, Tower and Hickey's Pond prospects, as the alteration signatures of each are similar.

The advanced argillic alteration, proximal to the Gold Hammer prospect, is the first example of this style of alteration identified within the volcanic rocks of the Long Harbour Group. Mapping of the alteration suggests that the two zones identified in Figure 6 may be linked, with the alteration in the area of the Gold Hammer prospect perhaps representing a lower temperature, more neutral pH environment. The apparent stratiform distribution of the advanced argillic alteration, within the volcanic sequence, displays similarities with that associated with the development of a lithocap, which is generally defined as being a horizontal to subhorizontal blanket of residual quartz and advanced argillic alteration above an intrusion (Sillitoe, 1995). But the development of pyrophyllite–diaspore alteration is generally indicative of higher temperatures within the deeper roots of a hydrothermal system (*e.g.,* Hedenquist and Taran, 2013). Nearby intrusions grouped as part of the Cross Hills Intrusive Suite are associated with extensive zones of pyritic alteration (*e.g.,* O'Brien *et al*., 1984), and could represent a potential heat source for the alteration and mineralization. However, geochronological data suggest that rocks assigned to the Cross Hills Intrusive Suite may not all be of the same age. The upper contact of this alteration with overlying siliciclastic sediments and related mafic flows and sills remains enigmatic, but if the clast of silica alteration identified in outcrop relates to the underlying epithermal system, an unconformable contact with overlying units is likely.

Several new zones of hydrothermal alteration in the Burin Peninsula area were identified through field work and follow-up of previous exploration sites, with some only evident through VIRS analysis. These are mostly barren, but anomalous values of As, Mo, Se and Te imply a broadly epithermal affinity (White and Hedenquist, 1995). The observed alteration within the area of White Mountain Pond is closely similar to that developed adjacent to the Forty Creek prospect (*cf.* Sparkes, 2012), which locally contains up to 59 g/t Au and 2290 g/t Ag (TerraX Minerals Inc., Press Release, December 20, 2010; Sparkes, 2012); however no such mineralization has yet been identified in the area of the White Mountain Pond alteration zone.

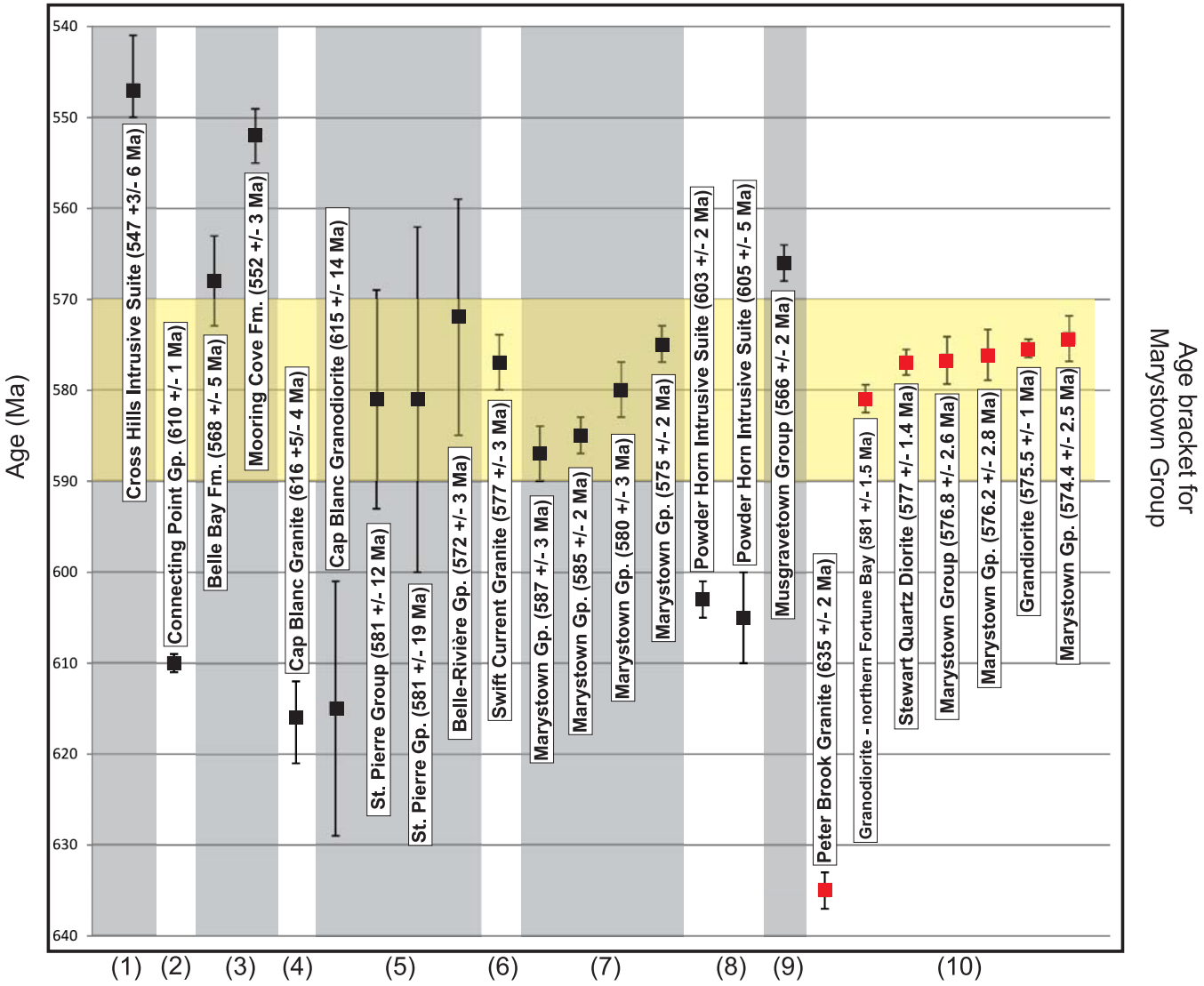


**Figure 10.** *Summary of available U/Pb geochronological data for the Burin Peninsula region and nearby St-Pierre and Miquelon. Also shown is the regional age bracket for the development of the Marystown Group. Numbers at the bottom of the plot refer to publications containing the relevant U/Pb zircon ages: 1) Tuach, 1991, 2) Dec* et al.*, 1992, 3) O'Brien* et al.*, 1994, 4) Dunning* et al.*, 1995, 5) Rabu* et al.*, 1996, 6) O'Brien* et al.*, 1998, 7) McNamara* et al.*, 2001, 8) Hinchey, 2001, 9) Clarke, 2012, 10)* this study.

## GEOCHRONOLGICAL RESULTS

The geochronological data presented generally support existing data, which are summarized in Figure 10, but also provide some new insights. The 635 ± 2 Ma intrusive rock from the Peter Brook prospect represents the first rock of this age identified on the Burin Peninsula. This is one of the oldest ages obtained from the entire region aside from those of the *ca.* 760 Ma Burin Group (Krogh *et al*., 1988; O'Brien *et al*., 1996). These results also provide a maximum age limit for the formation of the low-sulphidation veins at the Peter Brook prospect.

The 581 ± 1.5 Ma age from the granite obtained from the area west of Terrenceville indicates that rocks of similar age to the Swift Current Granite are present within areas currently included in the Cross Hills Intrusive Suite. The Swift Current Granite and correlatives are older than the *ca.* 570 Ma age for the base of the Long Harbour Group (O'Brien *et al.,* 1994), and therefore are unrelated to the formation of the advanced argillic alteration and related mineralization at the Gold Hammer prospect. Further work is required to better constrain the age of the Cross Hills Intrusive Suite and also to establish the relative extent of granitic units of different ages in this area.

The Stewart prospect is locally hosted by an altered quartz diorite dated at 577 ± 1.4 Ma, and now provides a maximum age limit on the formation of the advanced argillic alteration at the prospect. The alteration and related mineralization was interpreted as a collapsed porphyry system in which the advanced argillic alteration was superimposed on underlying porphyry-related mineralization (Dyke and Pratt, 2008). Dating of the altered quartz diorite and the adjacent Burin Knee granite demonstrates the two units are of essentially identical age, and both are correlative with the Swift Current Granite. The Burin Knee granite was previously correlated with the *ca.* 577 Ma Swift Current Granite by O'Brien and Taylor (1983), and the new data support this link.

Dating of the volcanic rocks at Lord's Cove, in the southern Burin Peninsula area, resolves some issues relating to the age of the Marystown Group. The age of 576.8 ± 2.6 Ma resembles those obtained from elsewhere within the region (Figure 10). The re-analysis of archived zircon from the sample TK77-23, originally described by Krogh *et al*. (1988), suggests that older inherited material was present in the earlier results, which account for the older age determination. New analyses from the sample using newer techniques now demonstrate the actual age of the sample to be 574.4 ± 2.5 Ma, which matches other reported ages from the Marystown Group. Investigation into the original sampling site for TK77-23 confirms the sample was actually collected 4.8 km east of the western Garnish exit (Figure 7; S.J. O'Brien, personal communication, 2013).

Finally, the age of 576.2 ± 2.8 for the volcanic rocks adjacent to the Tower prospect, indicates that these rocks are essentially of the same age as the *ca.* 572 Ma host rock to the Hickey's Pond prospect. Collectively, these results provide a maximum age limit on the formation of the advanced argillic alteration in the area. Unfortunately no units suitable for U/Pb age determinations are known to crosscut the alteration to provide a minimum age limit on its formation. The data are consistent with the original interpretation of O'Brien *et al*. (1999), in which the formation of the advanced argillic alteration in the area was suggested to be coeval with the intrusion of the 577 ± 3 Ma Swift Current Granite.

These new ages emphasize the period from 580 to 570 Ma as a period of active magmatism, which was probably accompanied by the formation of regionally extensive zones of advanced argillic alteration associated with the development of high-sulphidation systems. This period is closely similar to that suggested for the formation of the Hope Brook deposit (578–574 Ma; Dubé *et al*., 1998), and provides supporting evidence for an active period of hydrothermal activity throughout the Avalon Zone and related peri-Gondwanan arc terrains at that time.

## ACKNOWLEDGMENTS

We would like to thank Sarah Ferguson for her field assistance and insight, and Amanda Langille for excellent work in the U/Pb geochronology and Scanning Electron Microscope laboratories. Revisions by Andy Kerr greatly improved the clarity of the content.

## REFERENCES

Anderson, M.M., Bruckner, W.D., King, A.F. and Maher, J.B.

1975: The Late Proterozoic 'H.D. Lilly Unconformity' at Red Head, northeastern Avalon Peninsula, Newfoundland. American Journal of Science, Volume 275, pages 1012-1027.

Arribas Jr., A.

1995: Characteristics of high-sulphidation epithermal deposits, and their relation to magmatic fluid. *In* Magmas, Fluids, and Ore Deposits. Mineralogical Association of Canada Short Course Volume 23, pages 419-454.

AusSpec International Ltd.

2008a: Spectral interpretation field manual. Spectral analysis guides for mineral exploration. 3rd edition.

2008b: Practical applications handbook. Spectral analysis guides for mineral exploration. 3rd edition.

Black, L.P., Kamo, S.L., Allen, C.M., Aleinkoff, J.N., Davis, D.W., Korsch, R.J. and Foudoulis, C.

2003: TEMORA 1: a new zircon standard for Phanerozoic U–Pb geochronology. Chemical Geology, Volume 200, pages 155-170.

Blackwood, R.F. and Kennedy, M.J.

1975: The Dover Fault: Western boundary of the Avalon Zone in northeastern Newfoundland. Canadian Journal of Earth Sciences, Volume 12, pages 320-325.

Chang, Z., Hedenquist, J.H., White, N.C., Cooke, D.R., Roach, M., Deyell, C.L., Garcia Jr. J., Gemmell, J.B., McKnight, S. and Cuison, A.L.

2011: Exploration tools for linked porphyry and epithermal deposits: example from the Mankayan intrusion-centered Cu-Au district, Luzon, Philippines. Economic Geology, Volume 106, pages 1365-1398.

Clarke, M.

2012: Host lithologies, breccia development, alteration and gold mineralization at the Big Easy prospect. Unpublished B.Sc. thesis, Memorial University of Newfoundland, St. John's, Newfoundland, 85 pages.

Dallmeyer, R.D., Hussey, E.M., O'Brien, S.J. and O'Driscoll, C.F
1983: Geochronology of tectonothermal activity in the western Avalon Zone of the Newfoundland Appalachians. Canadian Journal of Earth Sciences, Volume 20, pages 355-363.

Dec, T., O'Brien, S.J. and Knight, I.
1992: Late Precambrian volcaniclastic deposits of the Avalonian Eastport basin [Newfoundland Appalachians]: petrofacies, detrital clinopyroxene geochemistry and paleotectonic implications. Precambrian Research, Volume 59, pages 243-262.

Degagne, P. and Robertson, D.J.
1985: Second year assessment report on geological and geochemical exploration for licence 2372 on claim block 1610 in the Monkstown Road area on the Burin Peninsula, southern Newfoundland. Newfoundland and Labrador Geological Survey, Assessment File 1M/09/0233, 39 pages.

Dimmell, P.
2003: First year assessment report on prospecting and geochemical and trenching exploration for licences 8377M and 9190M on claims in the Monkstown Road area, on the Burin Peninsula, Newfoundland. Newfoundland and Labrador Geological Survey, Assessment File 1M/09/0477, 25 pages.

Dimmell, P. and MacGillivray, G.
1989: First year assessment report on geological and geochemical exploration for licence 3433 on claim block 6099 in the Paradise River and Nine Island Pond areas on the Burin Peninsula, eastern Newfoundland. Newfoundland and Labrador Geological Survey, Assessment File 1M/09/0303, 42 pages.

Dubé, B., Dunning, G. and Lauziere, K.
1998: Geology of the Hope Brook Mine, Newfoundland, Canada: A preserved Late Proterozoic high-sulphidation epithermal gold deposit and its implications for exploration. Economic Geology, Volume 93, pages 405-436.

Dunning, G.R., Lepvrier, C., O'Brien, S.J., Colman-Sadd, S.P. and Maluski, H.
1995: Chronology of Avalonian events on the Presq'ile du Cap Miquelon (Le Cap), Saint-Pierre et Miquelon (France). Canadian Journal of Earth Sciences, Volume 32, pages 952-958.

Dunning, G.R., O'Brien, S.J., Colman-Sadd, S.P., Blackwood, R.F., Dickson, W.L., O'Neill, P.P. and Krogh, T.E.
1990: Silurian orogeny in the Newfoundland Appalachians. Journal of Geology, Volume 98, No. 6, pages 895-913.

Dyke, B.
2007: First, second, fourth and fifth year assessment report on prospecting and geochemical exploration for licences 9038M, 10975M, 11092M, 12650M and 12639M-12640M on claims in the Hickeys Pond and Powderhorn Hill areas, on the Burin Peninsula, Newfoundland. Newfoundland and Labrador Geological Survey, Assessment File 1M/0637, 60 pages.

2009: Second, third, fourth and seventh year assessment report on compilation and exploration history for licences 12650M, 13637M, 13640M, 15461M-15462M, 15963M-15964M and 15969M-15972M on claims in the Hickeys Pond area, on the Burin Peninsula, Newfoundland. Newfoundland and Labrador Geological Survey, Assessment File 1M/0687, 38 pages.

Dyke, B. and Pratt, W.
2008: First, second, third, fifth and sixth year assessment report on geological, geochemical and trenching exploration for licences 8405M-8406M, 8509M, 9038M, 10975M, 11092M, 12650M, 13189M, 13633M, 13637M-13640M, 14825M, 14827M and 14833M on claims in the Hickeys Pond and Powderhorn Hill areas, on the Burin Peninsula, Newfoundland. Newfoundland and Labrador Geological Survey, Assessment File 1M/0698, 317 pages.

Evans, D.T.W. and Vatcher, S.V.
2010: Second year assessment report on prospecting and geochemical exploration for licence 16483M on claims in the Lamaline area, on the Burin Peninsula, Newfoundland. Newfoundland and Labrador Geological Survey, Assessment File 1L/13/0211, 74 pages.

Hayes, J.P.
2000: First year assessment report on compilation, prospecting and geophysical exploration for licences 6420M-6421M, 6467M-6468M and 6623M on claims in the Monkstown Road area, on the Burin Peninsula, Newfoundland. Newfoundland and Labrador Geological Survey, Assessment File 1M/0537, 17 pages.

Hedenquist, J.H. and Taran, Y.A.
2013: Modeling the formation of advanced argillic

lithocaps: volcanic vapor condensation above porphyry intrusions. Economic Geology, Volume 108, pages 1523-1540.

Hinchey, J.G.
2001: An integrated geochemical, petrologic, geochronological, and metallogenic study of the Powder Horn Intrusive Suite and the associated Lodestar prospect – a magmatic-hydrothermal auriferous breccia zone that links epithermal and porphyry systems, northern Burin Peninsula, Newfoundland. Unpublished M.Sc. thesis, Memorial University of Newfoundland, St. John's, Newfoundland, 327 pages.

Huard, A.
1990: Epithermal alteration and gold mineralization in Late Precambrian volcanic rocks on the northern Burin Peninsula, southeastern Newfoundland, Canada. Unpublished M.Sc. thesis, Memorial University of Newfoundland, St. John's, Newfoundland, 273 pages.

Huard, A. and O'Driscoll, C.F.
1986: Epithermal gold mineralization in the late Precambrian rocks on the Burin Peninsula. *In* Current Research. Newfoundland Department of Mines and Energy, Mineral Development Division, Report 86-1, pages 65-78.

1985: Auriferous specularite-alunite-pyrophyllite deposits of the Hickey's Pond area, northern Burin Peninsula, Newfoundland. *In* Current Research. Newfoundland Department of Mines and Energy, Mineral Development Division, Report 85-1, pages 182-189.

Hussey, E.M.
2006: First year assessment report on compilation and geological and geochemical exploration for licence 10503M on claims in the Rocky Hills area, near English Harbour East, Fortune Bay, Newfoundland. Newfoundland and Labrador Geological Survey, Assessment File 1M/10/0574, 273 pages.

2009: Fourth year assessment report on geological and geochemical exploration for licence 15790M on claims in the Rocky Hills area, near English Harbour East, Fortune Bay, Newfoundland. Newfoundland and Labrador Geological Survey, Assessment File 1M/10/0676, 2009, 174 pages.

1979: The stratigraphy, structure and petrochemistry of the Clode Sound map area, northwestern Avalon Zone, Newfoundland. Unpublished M.Sc. thesis, Memorial University of Newfoundland, St John's, Newfoundland, 335 pages.

Jaffey, A.H, Flynn, K.F. Glendenin, L.E., Bentley, W.C. and Essling, A.M.
1971: Precision measurement of the half lives and specific activities of $^{235}U$ and $^{238}U$. Physical Review, Section C, Nuclear Physics, Volume 4, pages 1889-1906.

Kennedy, M.J., Blackwood, R.F., Colman-Sadd, S.P., O'Driscoll, C.F. and Dickson, W.L.
1982: The Dover-Hermitage Bay Fault: boundary between the Gander and Avalon Zones, eastern Newfoundland. *In* Major Structural Zones and Faults of the Northern Appalachians. *Edited by* P. St-Julyien and J. Beland. Geological Association of Canada, Special Paper Number 24, pages 231-247.

Kerr, A., Rafuse, H., Sparkes, G., Hinchey, J. and Sandeman, H. A.
2011: Visible/infrared spectroscopy [VIRS] as a research tool in economic geology: background and pilot studies from Newfoundland and Labrador. *In* Current Research. Government of Newfoundland and Labrador, Department of Natural Resources, Geological Survey, Report 11-1, pages 145-166.

Krogh, T.E.
1973: A low-contamination method for hydrothermal decomposition of zircon and extraction of U and Pb for isotopic age determinations. Geochimica et Cosmochimica Acta, Volume 33, No. 3, pages 485-494.

1982: Improved accuracy of U–Pb zircon ages by the creation of more concordant systems using an air abrasion technique. Geochimica et Cosmochimica Acta, Volume 46, pages 637-649.

Krogh, T.E., Strong, D.F., O'Brien, S.J. and Papezik, V.S.
1988: Precise U–Pb zircon dates from the Avalon Terrane in Newfoundland. Canadian Journal of Earth Sciences, Volume 25, pages 442-453.

Labonte, J.
2010: Fourth, fifth, seventh and eighth year assessment report on prospecting, reclamation and geochemical exploration for licences 12650M, 13637M and 15460M-15462M on claims in the Hickeys Pond and Powderhorn Hill areas, on the Burin Peninsula, Newfoundland. Newfoundland and Labrador Geological Survey, Assessment File 1M/0758, 87 pages.

Marsden, H. and Bradford, J.
2005: First year assessment report on geological and geochemical exploration for licence 11684M on claims in the Grand Beach area, on the Burin Peninsula, Newfoundland. Newfoundland and Labrador Geological Survey, Assessment File 1M/03/0555, 23 pages.

Mattinson, J.M.
2005: Zircon U–Pb chemical abrasion (CA-TIMS) method; combined annealing and multi-step partial dissolution analysis for improved precision and accuracy of zircon ages. Chemical Geology, Volume 220, pages 47-66.

McBride, D.
1987: Second year assessment report on geological and geochemical exploration for licence 2571 on claim block 3965 in the Sandy Harbour River area on the Burin Peninsula, eastern Newfoundland. Newfoundland and Labrador Geological Survey, Assessment File 1M/09/0266, 18 pages.

McNamara, A.K., Niocaill, C.M., Van der Pluijm, B.A. and Van der Voo, R.
2001: West African proximity of the Avalon terrane in the latest Precambrian. GSA Bulletin, Volume 113, No. 9, pages 1161-1170.

Myer, C. and Hemley, J.J.
1967: Wall rock alteration. *In* Geochemistry of Hydrothermal Ore Deposits. Holt, Rinehart and Winston, New York, pages 166-235.

O'Brien, S.J.
1993: A preliminary account of geological investigations in the Clode Sound-Goose Bay region, Bonavista Bay, Newfoundland [NTS 2C5/NW and 2D8/NE]. *In* Current Research. Government of Newfoundland and Labrador, Department of Mines and Energy, Geological Survey Branch, Report 93-1, pages 293-309.

2002: A note on Neoproterozoic gold, early Paleozoic copper and basement-cover relationships on the margins of the Holyrood Horst, southeastern Newfoundland. *In* Current Research. Government of Newfoundland and Labrador, Department of Mines and Energy, Geological Survey, Report 02-1, pages 219-227.

O'Brien, S.J., Dubé, B. and O'Driscoll, C.F.
1999: High-sulphidation, epithermal-style hydrothermal systems in late Neoproterozoic Avalonian rocks on the Burin Peninsula, Newfoundland: implications for gold exploration. *In* Current Research. Government of Newfoundland and Labrador, Department of Mines and Energy, Geological Survey, Report 99-1, pages 275-296.

O'Brien, S.J., Dubé, B., O'Driscoll, C.F. and Mills, J.
1998: Geological setting of gold mineralization and related hydrothermal alteration in late Neoproterozoic [post-640 Ma] Avalonian rocks of Newfoundland, with a review of coeval gold deposits elsewhere in the Appalachian Avalonian belt. *In* Current Research. Government of Newfoundland and Labrador, Department of Mines and Energy, Geological Survey, Report 98-1, pages 93-124.

O'Brien, S.J., Dunning, G.R., Knight, I. and Dec, T.
1989: Late Precambrian geology of the north shore of Bonavista Bay [Clode Sound to Lockers Bay]. *In* Report of Activities. Government of Newfoundland and Labrador, Department of Mines and Energy, Geological Survey Branch, pages 49-50.

O'Brien, S.J., Nunn, G.A.G., Dickson, W.L. and Tuach, J.
1984: Geology of the Terrenceville (1M/10) and Gisborne Lake (1M/15) map areas, southeast Newfoundland. Newfoundland Department of Mines and Energy, Mineral Development Division, Report 84-4, 54 pages.

O'Brien, S.J., O'Brien, B.H., Dunning, G.R. and Tucker, R.D.
1996: Late Neoproterozoic evolution of Avalonian and associated peri-Gondwanan rocks of the Newfoundland Appalachians. *In* Avalonian and Related Terranes of the Circum-North Atlantic. *Edited by* M.D. Thompson and R.D. Nance. Geological Society of America, Special Paper 304, pages 9-28.

O'Brien, S.J., O'Driscoll, C.F., Greene, B.A. and Tucker, R.D.
1995: Pre-Carboniferous geology of the Connaigre Peninsula and the adjacent coast of Fortune Bay, southern Newfoundland. *In* Current Research. Government of Newfoundland and Labrador, Department of Mines and Energy, Geological Survey, Report 95-1, pages 267-297.

O'Brien, S.J., O'Driscoll, C.F., Tucker, R.D. and Dunning, G.R.
1994: Late Precambrian geology and volcanogenic massive sulphide occurrences of the southwestern Avalon Zone, Newfoundland. *In* Report of Activities. Government of Newfoundland and Labrador, Department of Natural Resources, Geological Survey Branch, pages 77-81.

O'Brien, S.J., O'Neil, P.P. and Holdsworth, R.E.
1991: Preliminary geological map of part of the Glovertown [2D/9] map area, Newfoundland. Government of Newfoundland and Labrador, Department of Mines and Energy, Geological Survey Branch, Open File 2D/09/0260, [Map 91-169].

O'Brien, S.J., Strong, P.G. and Evans, J.L.
1977: The geology of the Grand Bank [1M/4] and Lamaline [1L/13] map areas, Burin Peninsula, Newfoundland. Government of Newfoundland and Labrador, Department of Mines and Energy, Mineral Development Division, Report 77-7, 19 pages.

O'Brien, S.J., Strong, D.F. and King, A.F.
1990: The Avalon Zone type area: southeastern Newfoundland Appalachians. *In* Avalonian and Cadomian Geology of the North Atlantic. *Edited by* R.A. Strachan and G.K. Taylor. Blackies and Son Ltd., Glasgow, pages 166-194.

O'Brien, S.J. and Taylor, S.W.
1983: Geology of the Baine Harbour (1M/7) and Point Enragee (1M/6) map areas, southeastern Newfoundland. Newfoundland Department of Mines and Energy, Mineral Development Division, Report 83-5, 70 pages.

Rabu, D., Thieblemont, D., Tegyey, M., Guerrot, C., Alsac, C., Chauvel, J.J., Murphy, J.B. and Keppie, J.D.
1996: Late Proterozoic to Paleozoic evolution of the St. Pierre and Miquelon islands: A new piece in the Avalonian puzzle of the Canadian Appalachians. *In* Avalonian and Related Terranes of the Circum-North Atlantic. *Edited by* M.D. Thompson and R.D. Nance. Geological Society of America, Special Paper 304, pages 65-94.

Reusch, D.
1985: First year assessment report on geological and geochemical exploration for licence 2571 on claim block 3965 in the Sandy Harbour River area on the Burin Peninsula, Newfoundland. Newfoundland and Labrador Geological Survey, Assessment File 1M/09/0243, 29 pages.

Reyes, A.G.
1990: Petrology of Philippine geothermal systems and the application of alteration mineralogy to their assessment. Journal of Volcanology and Geothermal Research, Volume 43, pages 279-309.

Saunders, P. and Reusch, D.
1984: First year assessment report on geochemical exploration for licence 2372 on claim block 1610 in the Paradise River and Monkstown Road areas on the Burin Peninsula, Newfoundland. Newfoundland and Labrador Geological Survey, Assessment File 1M/09/0225, 43 pages.

Seymour, C.R.
2006: Second and third year assessment report on prospecting and geochemical exploration for licences 10148M and 10928M on claims in the Long Harbour area, southern Newfoundland. Newfoundland and Labrador Geological Survey, Assessment File 1M/11/0585, 41 pages.

Sexton, A., Heberlein, K. and Thompson, A.J.B.
2003: First and second year assessment report on geological and geochemical exploration for licences 8102M, 8405M, 8509M, 8976M-8977M and 9039M on claims in the Paradise River area, on the Burin Peninsula, Newfoundland, 2 reports. Newfoundland and Labrador Geological Survey, Assessment File 1M/0468, 73 pages.

Sillitoe, R.H.
1995: Exploration of porphyry copper lithocaps. Australian Institute of Mining and Metallurgy, Public Series, Volume 9, pages 527-532.

Sparkes, G.W.
2012: New developments concerning epithermal alteration and related mineralization along the western margin of the Avalon Zone, Newfoundland. *In* Current Research. Newfoundland and Labrador, Department of Natural Resources, Geological Survey, Report 12-1, pages 103-120.

Sparkes, G.W., O'Brien, S.J., Dunning, G.R. and Dubé, B.
2005: U–Pb geochronological constraints on the timing of magmatism, epithermal alteration and low-sulphidation gold mineralization, eastern Avalon Zone, Newfoundland. *In* Current Research. Newfoundland Department of Mines and Energy, Geological Survey, Report 05-1, pages 115-130.

Stacey, J.S., and Kramers, J.D.
1975: Approximation of terrestrial lead isotope evolution by a two stage model. Earth and Planetary Science Letters, Volume 26, pages 207-221.

Stoffregen, R.E. and Cygan, G.L.
1990: An experimental study of Na-K exchange between alunite and aqueous sulfate solutions. American Mineralogist, Volume 75, pages 209-220.

Strong, D.F. O'Brien, S.J., Taylor, S.W., Strong, P.G. and Wilton, D.H.
1978a: Geology of Marystown (1M/3 and St. Lawrence 1L/14) map areas, Newfoundland. Newfoundland Department of Mines and Energy, Mineral Development Division, Report 77-8, 81 pages.

1978b: Aborted Proterozoic rifting in eastern Newfoundland. Canadian Journal of Earth Sciences, Volume 15, pages 117-131.

Thompson, A.J.B., Hauff, P.L. and Robitaille, A.J.
1999: Alteration mapping in exploration: Application of short-wave infrared (SWIR) spectroscopy. SEG Newsletter, Volume 39, pages 16-25.

Tuach, J.
1991: The geology and geochemistry of the Cross Hills Plutonic Suite, Fortune Bay, Newfoundland [NTS 1M/10], an Eocambrian to Cambrian alkaline gabbro–granodiorite–granite–peralkaline granite–syenite suite containing minor Zr–Y–Nb–REE mineralization. Government of Newfoundland and Labrador, Department of Mines and Energy, Geological Survey Branch, Report 91-2, 86 pages.

1984: Metallogenic studies of granite-associated mineralization in the Ackley Granite and the Cross Hills Plutonic Complex, Fortune Bay area, Newfoundland. *In* Current Research. Government of Newfoundland and Labrador, Department of Mines and Energy, Mineral Development Division, Report 84-1, pages 245-253.

White, N.C. and Hedenquist, J.W.
1995: Epithermal gold deposits: styles, characteristics and exploration. Society of Economic Geologists Newsletter, Number 23, pages 9-13.

Williams, H.
1979: Appalachian Orogen in Canada. Canadian Journal of Earth Sciences, Volume 16, pages 792-807.

1971: Geology of Belleoram map-area, Newfoundland. Geological Survey of Canada, Paper 70-65, 39 pages.

van Staal, C.R.
2007: Pre-Carboniferous tectonic evolution and metallogeny of the Canadian Appalachians. *In* Mineral Deposits of Canada: A Synthesis of Major Deposit-Types, District Metallogeny, the Evolution of Geological Provinces, and Exploration Methods. *Edited by* W.D. Goodfellow. Geological Association of Canada, Mineral Deposits Division, Special Publication No. 5, pages 793-818.